Assessment of the impact of urban block morphological factors on carbon emissions introducing the different context of local climate zones

Yuchen Qin [a,c], Jian Kang [d], Haizhu Zhou [e], Shen Xu [a,b,c,*], Gaomei Li [a,c], Chenqi Li [f], Wenjun Tan [a,c]

a. School of Architecture and Urban Planning, Huazhong University of Science and Technology, Wuhan, 430074, China

b. State Key Laboratory of Subtropical Building and Urban Science, Guangzhou, 510641, China

c. Hubei Engineering and Technology Research Center of Urbanization, Wuhan, 430074, China

d. Bartlett Faculty of Built Environment, University College London (UCL), London, WC1E 6BT, United Kingdom

e. China Academy of Building Research, Beijing, 100011, China

f. School of Architecture and Urban Planning, Shenyang Jianzhu University, Shenyang, 110168, China

E-mail addresses: xushen@hust.edu.cn (S. Xu).

Qin Y, Kang J, Zhou H, et al. Assessment of the impact of urban block morphological factors on carbon emissions introducing the different context of local climate zones. Sustainable Cities and Society, 2025, 119: 106073.

Abstract: Understanding the relationship between urban block morphology and carbon emissions is essential for developing effective low-carbon strategies, as it determines the buildings' contextual form and microclimate, substantially affecting buildings' energy demand. However, traditional indicators or typological methods define the buildings contextual form only through geometric features, which cannot fully reflect the complexities of urban environments and lack a unified spatial framework, hindering the establishment of standardized urban form-carbon emission mapping relationships. This study examines the compound effects of urban morphology on carbon emissions using a linear mixed-effects model, incorporating Local Climate Zones (LCZ) as the contextual form. The results demonstrate that LCZ explains 65.26% of the variation in carbon emission levels across blocks and significantly influences the relationship between urban morphology and carbon emissions. LCZ2 is one of the optimal low-carbon block morphological prototype. Building shape factor, height-to-width ratio, floor area ratio, building coverage ratio, and the facade area index are key design indicators that affect carbon emissions, with additional random effects as LCZ type changes. These findings suggest that the LCZ framework can help elucidate the relationship between block urban morphology, buildings contextual form and carbon emissions, and can be used to develop climate-responsive, low-carbon urban planning solutions.

Keywords: Local climate zone; Residential block carbon emission; Block urban contextual form; Urban morphology; The linear mixed model

Abbreviation

UBEM	Urban Buildings Energy Model
BES	Buildings Energy Simulation
CEI	Carbon Emission Intensity (Kg $CO^2/m^2/y$)
EUI	Energy Use Intensity($kWh/m^2/y$)
BSF	Building Shape Factor
H/W	Height-Width ratio
L/W	Length-Width Ratio
BCR	Building Cover Ratio
FAR	Floor Area Ratio
SVF	Sky View Factor
GSR	Green Space Ratio
BI	Buildings Interval
O	Orientation
BER	Buildings Enclosure Ratio
FAI	Frontal Area Ratio
PO	Porosity

1. Introduction

1.1. Background

As urbanization accelerates and global climate issues gain prominence, optimizing energy structures and managing carbon emissions in urban areas have emerged as critical challenges for all nations. Urban regions, despite covering only about 3 % of the Earth's surface, are responsible for approximately two-thirds of global energy consumption (Lombardi et al., 2017, Wang et al., 2020). Large-scale urbanization, industrial activity, and human behavior are primary drivers of energy use and carbon emissions, contributing to global climate change and resulting in adverse effects such as global warming and urban heat islands (UHI). These effects not only elevate health risks for residents but also escalate energy demand for urban activities, further increasing greenhouse gas (GHG) emissions, primarily CO^2. Such trends pose significant threats to social and environmental sustainability. Numerous researches have demonstrated that while various factors influence urban carbon emissions, urban morphology and the built environment are crucial determinants. These factors affect energy consumption directly through buildings and indirectly via transportation and industrial activities (Sharifi, 2019). Therefore, a strong correlation exists between urban morphology, land-use changes, and rising CO^2 levels (Jiang et al., 2020; Sun et al., 2022). Research indicates that optimizing urban form and building geometries can reduce energy consumption and carbon emissions by approximately 50 – 60%, addressing urban climate challenges (Zheng et al., 2022). In this context, the focus of urban development has shifted from large-scale suburban expansion to medium- and micro-scale urban form remodeling and community renewal. This approach aims to enhance land-use efficiency, optimize public facilities, and reduce motorized travel, thereby improving socio-economic outcomes and resource distribution. This shift is particularly relevant in large cities where urbanization has reached saturation. Blocks, as the smallest units of urban fabric, represent the fundamental scale and characteristics of urban form, functionality, and carbon-emitting activities, forming the foundation of urban life and energy use. Liu et al. identified that although blocks cover only 2.4% of global land, they account for approximately 80 % of energy consumption and carbon emissions (Liu et al., 2018). Consequently, blocks have become the primary focus of this phase of urban development. Urban block morphology—including buildings, green spaces, and transportation infrastructure—shapes the built environment and microclimate, significantly affecting energy consumption and carbon emissions. These features bridge the gap between building-scale and urban-scale energy systems, enabling the

analysis of interactions between buildings and their environments (Anderson et al., 2015). Therefore, urban blocks are critical for achieving low-carbon city objectives (Ye et al., 2023), and quantitatively analyzing their morphological factors is key to developing accurate carbon emission prediction models to reduce emissions and mitigate the UHI effect from an urban planning and design perspective (Wilson et al., 2008; Yang et al., 2018).

Building energy consumption, a major contributor to block-level carbon emissions, is influenced by the built environment and microclimate. The built environment — including building morphology, layout, and shading—regulates heat transfer, indoor lighting, and other fundamental energy uses, directly impacting carbon emissions (Xia & Zhang, 2018). Additionally, the block-level microclimate is closely linked to the block urban morphological features. Studies show that variations in the built environment and block morphology create distinct microclimate attributes, particularly in high-density urban areas (Chatterjee & Dinda, 2022). Increased urban construction intensity heightens environmental complexity and block variability, leading to disparities in surface heat fluxes. These disparities affect building energy demand, outdoor thermal comfort, and carbon metabolism, even between adjacent blocks, complicating energy management at the urban scale. This complicates energy management at the urban scale. Consequently, research on the relationship between urban morphological features, building carbon emissions, and urban contextual form must consider the interactions between the built environment and the microclimate. New metrics for defining the urban context of buildings are essential for comprehensively capturing the complexity of real-world urban blocks.

1.2. Literatures review

1.2.1. The effects of urban morphological factors on carbon emissions

Generally, building carbon emissions are generally evaluated using a full life-cycle approach, covering the design, construction, operational, and demolition phases. Among these, the operational phase contributes the largest share of carbon emissions, primarily driven by the energy demands of various equipment types. In comparison, embodied carbon emissions, which include those from construction, demolition, and the transportation of materials, typically represent less than 25 % of the total (Rock et al., 2020). Studies on individual building carbon emissions are typically not restricted to a specific phase, due to the relative ease of data acquisition and the limited scope of carbon emission calculations for individual buildings. Numerous studies have explored how factors such as building geometry, envelope characteristics, thermal properties, and materials influence carbon emissions at

different stages of a building's life cycle (Cang et al., 2020; Fang et al., 2021; Guo et al., 2024; Kamazani & Dixit, 2023; Wang et al., 2023; Mao et al., 2019; Zhang et al., 2024).

Life-cycle carbon emissions accounting demands significant data support, with research at city and block scales often concentrating on the operational phase. At the urban level, factors such as city size, population density, land use, transportation systems, and morphological changes driven by urban expansion significantly influence carbon emissions (Ao et al., 2022; Lan et al., 2023; Ma et al., 2015). Key urban morphology indicators include the scale and diversity of land use (Zhang et al., 2018), dispersion (Fang et al., 2015; Liu et al., 2020), compactness (Lee et al., 2015), three-dimensional spatial structure (Lin et al., 2021). In contrast, block-level carbon emission studies employ a broader range of methods. Besides traditional activity-based carbon accounting, direct measurements of CO^2 concentrations are often used to capture transportation-related emissions within blocks (CO^2 being the primary greenhouse gas in urban carbon emission researches) (Silva et al., 2022; Zhu et al., 2022). This approach has produced a richer body of research, revealing spatial-temporal patterns and relationships between carbon emissions and other environmental factors, such as pollutants and thermal environments (Liu et al., 2024; Mutschler et al., 2021). As the study scale narrows, carbon emission accounting shifts from supply-side factors to consumption-side metrics. Block-scale carbon emissions primarily encompass building energy use, transportation activities, waste treatment, and vegetation carbon sinks (Ji et al., 2022). Growing concerns about outdoor environmental quality and deteriorating urban climates have driven increased research attention to building density, land-use mixing, and block design, which can be controlled and optimized during planning. Urban morphological design indicators such as floor area ratio, land-use mix, street density, building type, and green space ratio are generally considered to be key factors influencing building-related carbon emissions (Bonenberg et al., 2023; Deng et al., 2016; Liu et al., 2023; Wang et al., 2011). He et al. investigated the impact of block density, shape indicators, and heterogeneity metrics — such as building height, footprint, aspect ratio, and surface-to-volume ratio—on operational carbon emissions (He et al., 2023). Allan et al. assessed the effects of urban densification strategies on both operational and embodied carbon emissions, arguing that considering emissions early in the design process significantly reduces overall emissions (Allan et al., 2022). Dong et al. studied the complex effects of geometric features (e.g., floor area, fractal dimension, and shape compactness), street networks, and spatial form, revealing that the same shape indicators influence carbon emissions differently in various geographic areas

(Dong et al., 2023). Liu et al. found that denser residential layouts reduce building energy consumption, thus lowering carbon emissions (Liu & Sweeney, 2012). While most studies on urban morphology and carbon emissions emphasize urban-scale characteristics and their direct effects, recent research has shifted towards block-scale mechanisms. This shift highlights the need to consider geographic location, block type, microclimatic phenomena, and the rationale behind selecting morphological indicators of the built environment.

1.2.2. The effect of urban climate conditions on the buildings energy consumption and carbon emissions

Numerous studies have already demonstrated that the microclimate environment is an important mediator in the process by which urban morphology influences building energy consumption and carbon emissions (Pasandi et al., 2024). The complex characterization of built environments in near-surface blocks affects convective heat transfer processes, influencing air temperature, relative humidity, wind conditions, and building exterior surfaces. This, in turn, impacts outdoor environmental conditions, energy use, and carbon emissions. The interaction mechanism of "urban morphology-microclimate-building energy performance" can be studied through two research pathways at different levels of analysis. The "urban morphology-microclimate/environmental performance" path, which focuses on direct relationships, has been extensively explored. Many studies examine how street-level geometry (e.g., orientation, aspect ratio, height-to-width ratio) and urban form (e.g., building coverage ratio, height distribution) influence microclimatic factors and environmental comfort, such as thermal and wind comfort (Ali-Toudert & Mayer, 2006; Banerjee et al., 2024; Ma et al., 2022; Yang et al., 2017). The "urban morphology-microclimate-building performance" path is more complex, examining how urban form and microclimate jointly impact energy consumption through field studies, big data analysis, or simulations in diverse climate zones or microclimatic settings. Revealing the interactions between urban morphology, microclimate, and building energy characteristics remains an issue of interest, considering aspects such as the choice of microclimate measurement methodology and the definition of the research problem. Athar et al. verified the validity of the microclimate meteorological data in the Marina district in the city of Lusail near Doha, Qatar, exploring the impact of urban form on the microclimate as well as on the local energy loads of buildings (Kamal et al., 2021). Zheng et al. explored the relationship between old settlements in cold areas, building patterns and carbon emissions at the block-scale during the operation phase of the buildings (Zheng et al., 2023); Xuan et al. examined how

spatial layouts affect wind and thermal environments, proposing strategies to enhance microclimates and reduce energy consumption in residential blocks (Xuan, 2021). It can be found that microclimate is commonly used as a framework for assessing building energy use and carbon emissions, as it comprehensively reflects the interaction between building form, surface environment, and weather conditions. However, the existing literature has shown that both empirical measurements and simulations struggle to comprehensively define the spatial scope of microclimates within urban blocks, particularly in studies involving microclimate assessments. This makes it challenging to compare microclimatic variations between different blocks and their dynamic correlations with energy demand. Given the complex and variable surface conditions of the urban boundary layer, significant differences in heat flux can occur within a block, which can further exert substantial impacts on both environmental and building performance. Thus, it is necessary to conduct further research in this area.

1.2.3. The defining method of the buildings urban contextual form for carbon emission studies

Urban contextual form measurement is a key issue in studying the relationship between urban morphology and building energy performance. This challenge revolves around methodological considerations on how to effectively define urban environments and whether such approaches can sufficiently capture the complexity of real-world urban environments. Traditional studies frequently rely on independent 3D models for energy simulations, but whether realistic or generic, these models often fail to fully represent the intricacies of real urban forms (Gobakis & Kolokotsa, 2017; Li et al., 2024; Rostami et al., 2024; Yang et al., 2024). As a result, when researchers define environmental contexts for building energy studies, they usually focus on the geometric characteristics of individual buildings themself, though the methods for defining these characteristics differ. Many studies use design indicators like density, geometric metrics, morphology typology, or land use and land cover(LULC) to define the urban contextual form (Quan & Li, 2021). However, these approaches only capture specific aspects of urban form in restricted dimension. Furthermore, inconsistencies in calculation methods and spatial boundaries across various indicators lead to variations in how individual morphological factors influence block environmental performance (Ahn & Sohn, 2019; Shen et al., 2024). Introducing more complex indicators to define building groups from multiple perspectives can provide a more comprehensive representation of spatial form characteristics. However, it becomes increasingly challenging to succinctly compare the relationship between

urban form characteristics and building energy performance across different urban zones, and translate these insights into urban planning and design management. Another widely adopted approach is to define morphological characteristics through typology. This method abstracts and simplifies the complex features of urban environments and morphology into a representative formal language. Martin and March developed the urban form prototypes method, which have been applied in studies examining urban form and building energy consumption (Martin & March, 1972). Despite being more integrated and comprehensive than the indicator-based approach, this method remains insufficient in accurately representing the buildings contextual urban environment, especially regarding the climatic context and its influence on building energy consumption.

The “Local Climate Zones” classification system, developed by Stewart and Oke, is a crucial tool in urban climatology for analyzing local temperature variations across diverse measurement sites (Stewart & Oke, 2009). Microclimate, resulting from the interaction of meteorological conditions and urban physical structures, serves as a contextual backdrop for this analysis. The LCZ method effectively captures and visualizes this interplay through a typological lens, offering a standardized database of urban forms categorized by various environmental elements, including ground materials, water, and vegetation. Initially designed to differentiate between urban and rural forms in studying the urban heat island effect (Parvar et al., 2024), the LCZ typology incorporates aspects of urban morphology and landscape factors such as sky visual coefficients, aspect ratios, and building surface characteristics. This allows it to characterize different microclimates within the same area, making it an ideal context for examining the relationship between urban morphology and building energy performance, which base on the interplay of microclimate, urban form and building energy relations. Wu et al. utilized the LCZ framework to map carbon emission regions in Shanghai, enhancing the granularity of urban-scale carbon emission studies (Wu et al., 2018). Yang et al. explored energy consumption patterns across various microclimate scenarios, finding that cumulative energy use is higher in compactly distributed buildings compared to those in more open arrangements (Yang et al., 2020). Mouzourides et al. proposed a systematic approach for transforming geographically-based data into a comprehensive grid of numerical information using the LCZ framework, applying this method to investigate the link between urban form and carbon emissions in London (Mouzourides et al., 2019). While these studies addressed variations in urban heat island intensity and building energy behavior across different LCZs, they did not consider urban form as a covariate nor did they examine the differences in urban morphological factors across various LCZ zones.

1.3. Research motivations and contributions

Defining the urban contextual form of buildings within blocks is crucial for the efficacy of form-energy demand mapping models in urban planning and design. However, research on how surrounding environments influence this relationship remains limited. Traditional methods that rely on urban morphology to define contextual environments focus primarily on geometric forms and often neglect microclimate factors, failing to capture the complexity of block-scale environments (Barone et al., 2024; Li & Quan, 2024; Quan et al., 2020; Song et al., 2024). These methods require clearly defined spatial scopes, suitable indicators, and complex computational models, which vary across studies—ranging from general descriptions to diverse research approaches depending on the analysis objectives (Adolphe, 2001; Oliveira, 2022; Fleischmann et al., 2021). Furthermore, numerous block examples are required to substantiate the rationale for generalizing urban environments based on typical block patterns. Analyzing microclimate characteristics also relies on simulation software, complex parameterization, and significant computing resources (Liu et al., 2021; Tu et al., 2023). Differences in methods for calculating environmental form features hinder the integration of built form and physical environment when defining block contexts, despite their significant interactions, particularly concerning building energy use. The neglect of the systemic wholeness of block environments leads to a disconnection from real urban conditions, making it challenging to apply the findings in urban planning and management. The absence of a unified definitional framework causes many studies to focus on isolated features, often neglecting spatial interactions between environmental characteristics, depending on the study's focus (Wang et al., 2024). The Local Climate Zone (LCZ) framework offers a standardized method for describing the morphological features of urban areas and their thermal environments at the block level, addressing some limitations of previous research (Li et al., 2024). Although early studies have proposed using this framework to classify urban morphology types and investigate factors influencing building energy demand, they often focus on phenomena at the city scale. These studies typically do not account for detailed block-level morphological factors as covariates, nor do they analyze the compound effects and interactions with different LCZ types in depth. Given these gaps, this study aims to thoroughly analyze the mechanisms by which various block-scale urban morphological factors influence carbon emissions, considering the LCZ framework. The research will quantify these relationships and explore how they vary across different LCZ types, ultimately developing an accurate spatial mapping model that links urban form, microclimate

conditions, and carbon emissions. The primary contributions of this study are as follows:

(1) Utilizing the LCZ framework to define urban contextual forms, thereby capturing the complexity of the "built environment microclimate-carbon emission" coupled system and enhancing understanding of carbon emissions distribution across urban forms and environmental levels.

(2) Introducing additional indicators for block- and building-scale morphological factors as covariates, and verifying the fixed and random effects of these factors on block carbon emissions using a linear mixed regression model influenced by LCZ. This approach enhances the granularity of the analysis regarding urban morphology and carbon emissions.

(3) Proposing a standardized scheme for developing an urban carbon emission zoning model and a method for urban form design regulation aimed at mitigating carbon emissions, emphasizing its integration with traditional planning and design tools.

We will first introduce the study area and research samples, detailing the creation of standardized LCZ maps, the selection of target block cases, and the determination of block-level urban morphological indicators. Next, we will outline the simulation methods employed using Rhino and Grasshopper, the approach for calculating carbon emissions, and the linear mixed-effects model (LMM) used for data analysis. Based on the results of the multi-level model analysis, we will discuss carbon emission levels and disparities across different LCZ types, as well as the relationships between urban morphology parameters and carbon emissions within each LCZ. Finally, by integrating our model analysis findings with recent studies on the relationship between LCZ and building energy demand, we will address two key aspects: (1) the integration of LCZ-based urban carbon emission mapping methods with traditional urban planning zoning tools and energy policies, and (2) regulatory strategies for urban form design aimed at reducing carbon emissions across different LCZ zones. (Fig. 1)

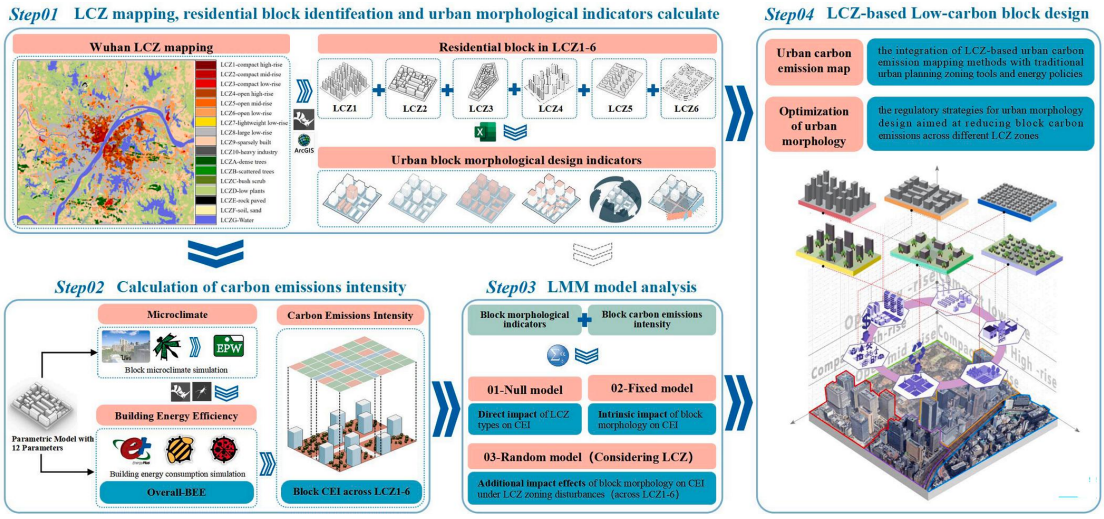

Fig. 1. Research framework.

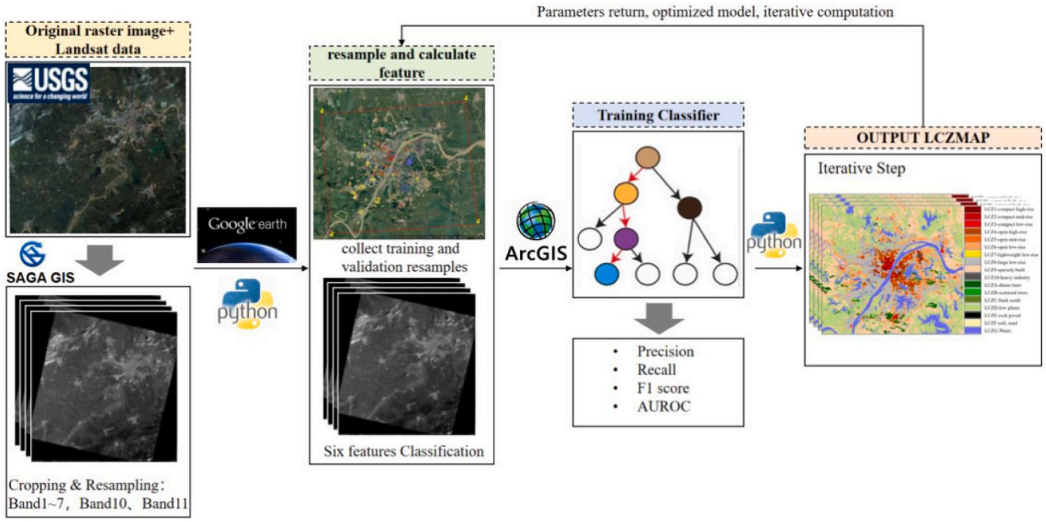

Fig. 2. LCZ map construction methods.

2. Study area, data, and methods

2.1. Study area

Wuhan, located in central China, is a significant urban center within a typical hot-summer, cold-winter (HSCW) climate zone. By the end of 2023, the city's urbanization rate is expected to reach 84.79 %, with further growth anticipated. This urban expansion, coupled with population growth, is likely to drive up carbon emissions due to intensified construction activities. Additionally, Wuhan's HSCW climate is characterized by prolonged periods of high temperatures in both summer and winter, along with cold and humidity, which greatly heighten building energy demand. Given Wuhan's representative climatic conditions and energy requirements, an LCZ-based investigation into the relationship between urban form characteristics and carbon emissions can significantly enhance the integration of urban climatic

factors and energy dynamics into planning and design. This integration is essential for developing climate-resilient cities and improving the quality of life for residents.

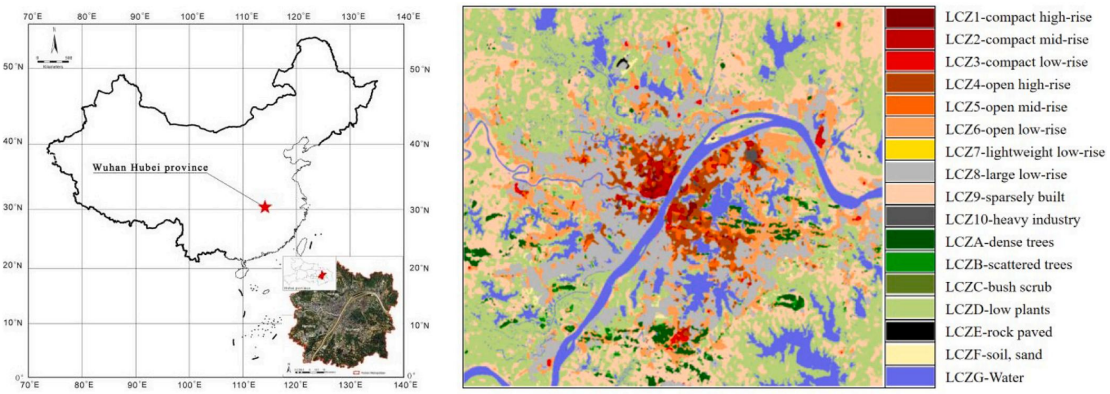

Fig. 3. LCZ Map, Wuhan, Hubei Province, China.

Before initiating the research, several preconditions must be established: 1) Based on the spatial form classification of LCZ and their index intervals, as outlined by Stewart, it is clear that LCZ7-10 have a limited number of buildings. Consequently, this study concentrates on LCZ1-6, which include compact high-rise, compact mid-rise, compact low-rise, open high-rise, open mid-rise, and open low-rise zones; 2) The analysis is restricted to the carbon emissions of residential blocks. This focus is justified by the substantial size and broad scope of these blocks, which are closely tied to residents' lives and have significantly higher energy consumption compared to other building types. Their energy-saving potential is considerable, and they also feature relatively straightforward performance parameters—such as the enclosure structure, equipment, and residents' energy usage behaviors—facilitating the subsequent simulation of building energy consumption.

Given the complexities associated with the implementation and application of various LCZ methods, this study employs remote sensing satellite imagery to create a standardized LCZ map for Wuhan (Gamba et al., 2012; Stewart & Oke, 2012; Zheng et al., 2018). Following the procedures outlined by the World Urban Database and Access Portal Tool (WUDAPT), the Landsat 8-9 OLI/TIRS C2 L1 dataset from the USGS (http://glovis.usgs.gov/) was utilized as the primary source for remote sensing data. Typical daily satellite images from both summer and winter of 2023 were collected and integrated to produce a comprehensive LCZ map of the city. The satellite data were resampled using SAGAGIS and ARCGIS, adjusting the original 30 ×30 m resolution to 100 m. These resampled data were projected onto the WGS84/UTM50N coordinate system and used for subsequent classification and supervised learning to delineate the LCZs, resulting in the standard LCZ maps (Fig. 2). In previous studies conducted by various scholars across different cities, unit sizes were typically set at 100 m and 50/100 m intervals. The optimal size was determined

by analyzing basic spatial attributes related to air temperature variations. The minimum radius for sample zones was generally within the range of 100-500 m (Huang et al., 2018). This study selected five scales—100 m, 200 m, 300 m, 400 m, and 500 m—for generating sample zones. Additionally, based on China's "Standard for Urban Residential Area Planning and Design" and the specific context of Wuhan's residential blocks, the basic raster unit was determined to be 200 m. Consequently, complete residential areas were delineated according to road boundaries as samples. The final LCZ zoning map of Wuhan is shown in Fig. 3.

A total of 120 residential block samples from LCZ 1 to 6 zones were selected for the study through fieldwork and an online street map survey. The block 3D models were constructed using building footprint data and height data downloaded from the official OpenStreetMap (OSM) website. These 3D models were then aligned with the latest Baidu satellite maps and street maps to calibrate the building contours, 3D shapes, and number of floors to reflect real-world conditions. Finally, a block building model was created on the Rhino platform for subsequent energy simulation and carbon emission calculation. The typical spatial patterns of the blocks and other built environment indicators for each LCZ zone are shown in Table 1.

Table 1 Residential block sample in LCZ1-6.

LCZ Types	Spatial attribute values	Typical residential block styles	Block 3D model
LCZ1: Compact high-rise 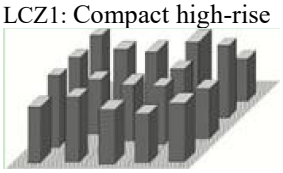	BH: 70.45-120.61m SVF: 0.182-0.353 FAR: 10.57-20.43 BCR: 0.271-0.353 H/W: 1.71-2.53	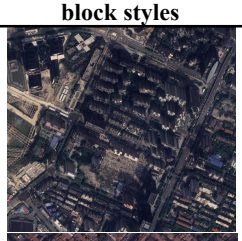	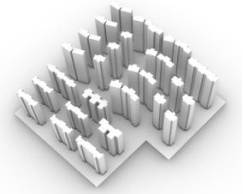
LCZ2: Compact mid-rise 	BH: 18.65-30.50m SVF: 0.195-0.502 FAR: 3.59-9.87 BCR: 0.315-0.380 H/W: 0.75-1.66	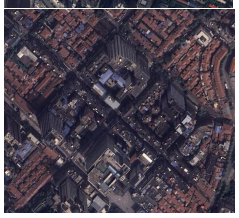	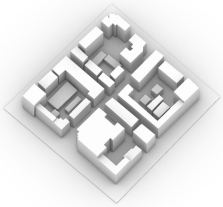
LCZ3:Compact low-rise 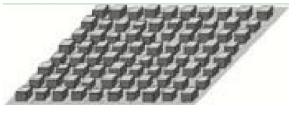	BH：6.71-9.08m SVF：0.302-0.579 FAR：1.67-4.42 BCR: 0.305-0.452 H/W：0.75-1.5		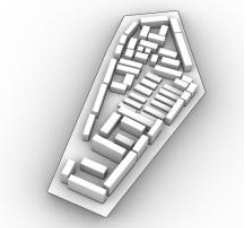
LCZ4:Open high-rise 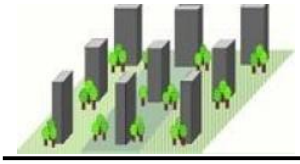	BH：60.10-75.52m SVF：0.125-0.301 FAR：7.85-12.41 BCR: 0.201-0.277 H/W：0.75-1.25		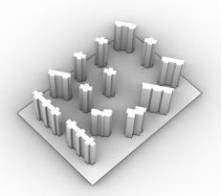

LCZ5:Open mid-rise 	BH：15.85-23.12m SVF：0.42-0.601 FAR：0.84-2.55 BCR: 0.182-0.260 H/W：0.3-0.75	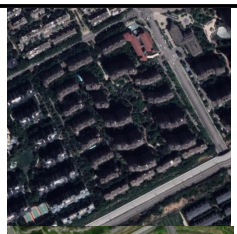	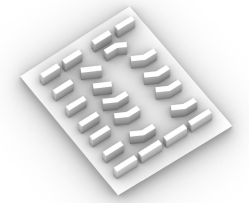
LCZ6:Open low-rise 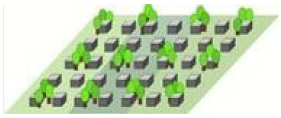	BH：4.50-10.70m SVF：0.626-0.805 FAR：0.14-0.39 BCR: 0.121-0.248 H/W：0.3-0.75		

2.2. Urban morphological indicators

Urban morphological indicators were selected to characterize urban block form by considering two pathways through which urban form impacts building energy consumption and microclimate (Cui et al., 2024; Natanian & Wortmann, 2021; Xu et al., 2024), as well as the potential confounding effects of urban morphological factors inherent in the LCZ definition method. The three primary morphological indicators defining LCZ form are building cover ratio, building height, and sky view factor. Of these, building height directly influences the vertical characteristics of LCZs. To ensure consistency in thermal environment characteristics within a given LCZ, building heights within standardized spatial units are maintained within a uniform range. Minor variations in building height within the same LCZ type are acceptable. Due to the high auto-correlation between LCZ type and building height, building height was excluded as a morphological indicator to prevent compromising the model's performance when considering LCZ type as a main effect. After consulting relevant literature (Du et al., 2024; Peng et al., 2024), this study identifies building-scale morphological indicators, such as the building shape factor, height-to-width ratio, and length-to-width ratio. Block-scale morphological factors, including floor area ratio, building cover ratio, green space ratio, building enclosure ratio, orientation sky visibility factor, and building interval, were also selected. Additionally, microclimatic correlates of morphological factors, such as frontal area ratio and porosity, are incorporated into the analysis (Leng et al., 2020; Liu et al., 2023; Zhou & Zhang, 2021). To ensure a balanced assessment of how the three-dimensional building shapes within a block influence key indicators that require averaging, a weighted approach is employed. Specifically, overall building dimensions (height, width, depth), aspect ratios, depth ratios, and other shape factors are weighted based on total volume (Table 2).

Table 2 Urban morphological factors and graphical representation.

Indicators type	Formula	Interpretation	Graphical representation
Building-scale morphological factors	$BSF = \frac{S_b}{V_B}$	S_b is the sum of the individual building exterior area. V_B is the sum of the individual building volume.	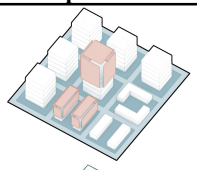
	$H/W = \frac{\sum_{i=1}^{n} h_i V_i}{\sum_{i=1}^{n} V_B} / \frac{\sum_{i=1}^{n} w_i V_i}{\sum_{i=1}^{n} V_B}$	h_i is the height of the building i. V_i is the volume of the building i. w_i is the width of the building i. Other parameters have the same meaning as above	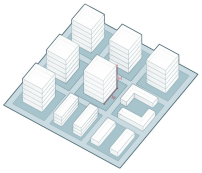
	$L/W = \frac{\sum_{i=1}^{n} l_i V_i}{\sum_{i=1}^{n} V_B} / \frac{\sum_{i=1}^{n} w_i V_i}{\sum_{i=1}^{n} V_B}$	l_i is the length of the building i. Other parameters have the same meaning as above	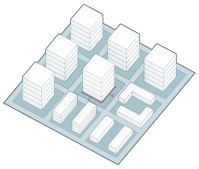
	$FAR = \frac{S_A}{S_G} \times 100\%$	S_A is the the total floor area of the buildings. S_G is the total site area of the block	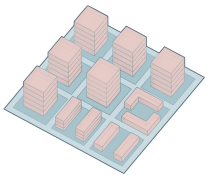
	$BCR = \frac{S_D}{S_G} \times 100\%$	S_D is the sum of the base area of all the buildings in the block.Other parameters have the same meaning as above	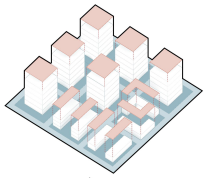
	$GSR = \frac{S_g}{S_G} \times 100\%$	S_g is the sum of the area of green space in the block. Other parameters have the same meaning as above	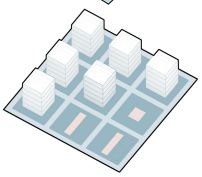
Block-scale morphological factors	$SVF = \frac{R_P}{R_G}$	R_P is the solar radiation received from the visible sky at a point in block. R_G is the global horizontal radiation received by the unobstructed hemisphere of the sky	
	$BI = \frac{\sum_{i=1}^{n} L_i}{n} \times 100\%$	D_i is the distance to the windward face of the building i (when the buildings are not parallel, take the average of the sum of the maximum and minimum values of the spacing).	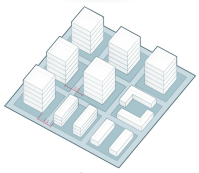
	$O = \frac{\sum_{i=1}^{n} Q_i V_i}{n \times \sum_{i=1}^{n} V_B}$	Q_i is the orientation of the individual building i. Other parameters have the same meaning as above	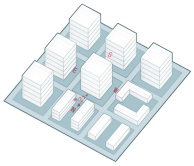
	$BER = （L_1 + L_2 + \ldots + L_i）/L$	L_i is the perimeter of the building facade in the block. L is the total length of the interface along the street in the block	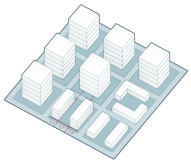

$FAI = \frac{S_F}{S_T}$	S_F is the area of the front windward area of the building in F wind direction.Other parameters have the same meaning as above	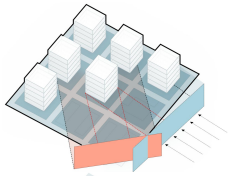
$P_o = \frac{\sum_{i=1}^{m} V_i}{V_B}$	V_i is the volume of the urban canopy segment i. Other parameters have the same meaning as above	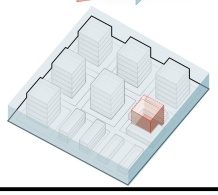

2.3. Calculation of the carbon emissions intensity at the block-scale

2.3.1. Calculation of the block carbon emissions

As previously noted, the operational phase of a building is the primary contributor to carbon emissions throughout its life cycle, with electricity consumption and natural gas usage being the main factors (GBT 51366-2019 2019). A survey of energy usage among residents in Wuhan indicated that electricity consumption is approximately nine times greater than that of gas, while water usage contributes minimally to overall emissions. Additionally, due to the difficulties in obtaining measured data for simulating tools, this study will concentrate on two main categories of carbon emission accounting: (1) emissions from daily electricity consumption during the operational phase, specifically related to HVAC systems, lighting, and other electrical systems; and (2) carbon sinks resulting from block greening throughout the building's life cycle. Transportation-related emissions are excluded from this study due to challenges in forecasting motor vehicle traffic at the block scale and its strong correlation with geographic location.

Given the significant variability in environmental and morphological characteristics across different blocks, a direct comparison of carbon emissions among buildings without standardized criteria is impractical. Therefore, following energy calculations, we will conduct a detailed analysis of energy consumption using the Carbon Emission Intensity (CEI) method (Eq. (1)). This approach will allow us to clarify differences in carbon emissions among buildings within various blocks. The formulas relevant to this study's definition of carbon emission accounting for residential blocks are as follows:

$$CEI = \frac{\sum_{i=1}^{n} E_{ei} \times f_E - E_L}{A} \tag{1}$$

$$E_L = \sum_{t=1}^{t} Q_t \times \mu \times EF_N \tag{2}$$

$$EUI = \frac{E_{ei}}{A} \tag{3}$$

CEI is the annual building carbon emissions intensity per unit of building area (kg $CO^2/m^2/y$). E_{ei} is the whole-year building energy consumption of the residential blocks (including the energy consumption for cooling, heating, lighting, and electrical equipment (kWh/y), i represents category i electricity demand), f_E is the electric power carbon emissions factor (which was 0.801 kg/kWh) (National Development & Reform Commission 2011). A is the total floor area of the residential block (m^2). E_L is the annual carbon reduction in the building's green space carbon sink system (kg CO^2/y). Q_t is the area of the different planting methods (m^2), η is the ratio of the tree cover (which is 30 % (Ye & Wang, 2015)), and EF_N is refers to the carbon sink factors of different planting methods (which is 0.112 $kgCO^2/m^2/y$ (Wang, 2010)). EUI is the annual energy use intensity per unit of building area ($kWh/m^2/y$).

2.3.2. Building energy simulation

Simulating energy consumption in block-scale building clusters requires consideration of shading relationships among buildings, the surrounding environment, and the ability to perform batch calculations on large samples. To integrate 3D modeling with energy simulation, we selected Rhino software alongside built-in plugins like Ladybug and Honeybee within the Grasshopper platform, utilizing the Energy Plus engine for microclimate and operational energy simulations.

To accurately represent microclimatic conditions across different LCZ zone, we substituted traditional EPW files with microclimate data specifically designed for the thermal characteristics of each zone. Standard EPW files, which generally reflect urban-scale meteorological conditions from outskirts weather stations, do not adequately capture block-level microclimates. Microclimate simulation was conducted using the Dragonfly plugin for Rhino & Grasshopper, employing the UWG engine to link meteorological data from Wuhan with CSWD sources. Based on the standard spatial attribute ranges for LCZs 1-6, combined with field research and street maps, we obtained the spatial morphology of these zones. Using ArcGIS software and Grasshopper, we compiled basic spatial morphology attributes and established essential parameters for the LCZ, including urban morphology and landscape distribution characteristics, as well as three thermal environment parameters (thermal, radiative, and metabolic). The modified UWG file was then input into the Energy Plus simulation engine as the meteorological file for energy analysis. Fig. 4 illustrates the calculation process for building energy simulation and carbon emissions.

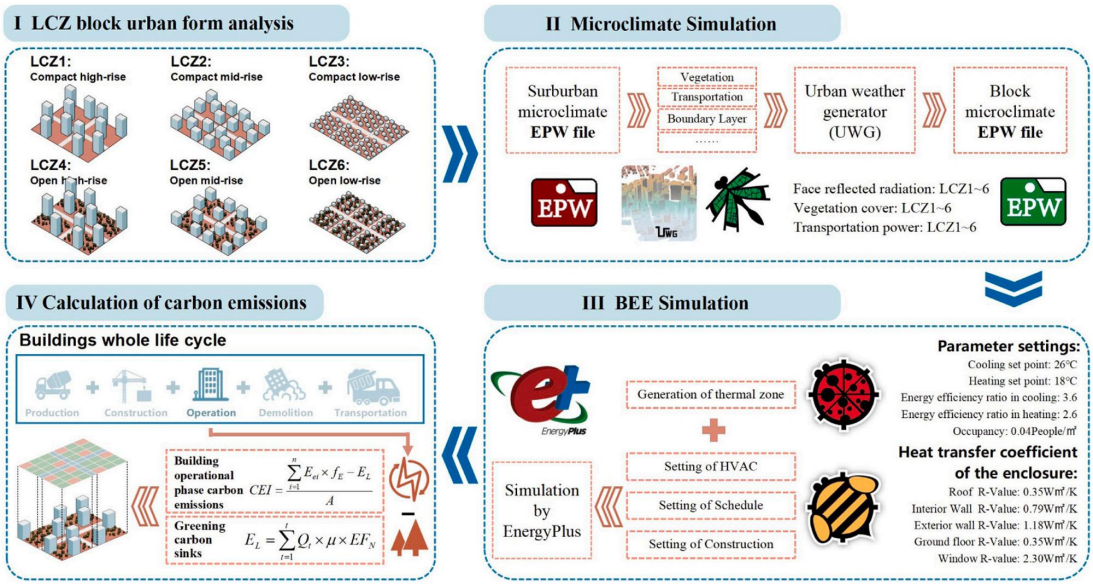

Fig. 4. Calculation of CEI during the operational phase of the block.

The relevant BES model parameters (room occupancy rate, set temperature, power of lighting and heating equipment, etc.) and the window-to-wall ratio are set with reference to the China's Technical standard for nearly zero energy buildings (GB/T 51350-2019), Design standard for energy efficiency of residential buildings in hot summer and cold winter zone (JGJ 134-2010), Design standard for residential buildings of low energy consumption (DB 42/T559-2013), the Design standard for energy efficiency of residential buildings in hot summer and cold winter zone (JGJ 134-2010) and the typical residential practice project energy saving report research results (Tables 3–5).

Table 3 Basic Parameter setting in the BES model-1

operating parameter	Indoor set temperature during the heating period	Indoor set temperature during cooling period	Human body heat load	Lighting power density	Equipment power density
setpoint	18℃	26℃	108W/person	3W/㎡	4W/㎡
Data sources	JG134-2010		JGJ/T449-2018	Validation of corrections	experimental
		Occupancy Rate			
8a.m.-7p.m. Monday-Friday	8a.m.-9a.m. 0.17	9a.m.-12a.m. 0.96	12a.m.-1p.m. 0.04	1p.m.-2p.m. 0.81	2p.m.-6p.m. 0.96	6p.m.-7p.m. 0.23
9a.m.- 5p.m. Saturday-Sunday	8a.m.-9a.m. 0.10	9a.m.-12a.m. 0.18	12a.m.-1p.m. 0.04	1p.m.-2p.m. 0.04	2p.m.-6p.m. 0.18	6p.m.-7p.m. 0.10

Table 4 Basic Parameter setting in the BES model-2

Building orientations	window-wall ratio		window sill	Window height	floor height
	setpoint	Limits			
N	0.25	≤0.3	0.9m	1.5m	3m
W	0.2	≤0.3	0.9m	1.5m	3m
S	0.3	≤0.35	0.9m	1.5m	3m
E	0.2	≤0.3	0.9m	1.5m	3m

Table 5 Basic Parameter setting in the BES model-3

Enclosure		Set value of the integrated heat transfer coefficient L/[W/（㎡·K）]
Transparent enclosure	Window	2.30
Non-transparent enclosures	Roof	0.35

Exterior wall	1.18
Floor slab	1.14
Interior wall	0.79

2.3.3. The validation of the BES

The validation of building energy simulations, accounting for microclimate influences, involved a detailed comparison between actual energy consumption data from residential blocks and corresponding monthly software simulation results. To accurately reflect the real-world conditions of residential blocks in Wuhan, a comprehensive survey was conducted with 49 randomly selected residents from a large-scale development to assess their electricity consumption patterns. The average values from this survey were used to calculate both the annual energy consumption for the community and the monthly usage patterns. Subsequently, the energy simulation process commenced, with modifications to lighting power and other equipment in response to reduce the difference between simulated and actual values. This iterative adjustment process continued until satisfactory alignment between the simulated and measured data was achieved. Initially, while the simulation and actual consumption exhibited similar trends, significant deviations persisted. An analysis of floor layouts and indoor energy use patterns in Wuhan highlighted the need to recalibrate unit power densities for lighting and other equipment (see Fig. 5). Ultimately, after refining these power values, the error margin for the measured annual energy consumption was reduced to 8.57 %, with the measured Energy Use Intensity (EUI) at 32.15 kWh/m²/y and the simulated value at 29.61 kWh/m²/y.

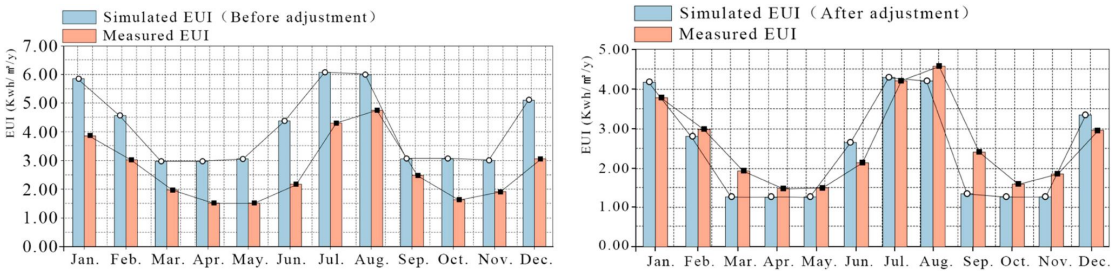

Fig. 5. Comparison of simulated and measured energy consumption.

2.4. Data analysis method

The linear mixed-effects model is utilized to examine both fixed and random effects of urban morphological factors at the block scale on carbon intensity, considering the influence of LCZ. This study employs three tiers of process models: the null model, fixed-effects model, and random-effects model. The null model evaluates overall differences in carbon emission levels across all samples, investigates variations among residential blocks in different LCZ zone, and analyzes spatial

aggregation patterns. This initial analysis identifies any significant intervening effects related to LCZs and assesses the consistency of carbon emissions across various types, providing a foundation for further effect modeling. The fixed-effects model evaluates the intrinsic influence of morphological parameters on CEI, excluding LCZ considerations, thereby reflecting inherent morphological impacts independent of the built contextual form. The random-effects model accounts for the added influence of morphological factors on CEI across different LCZ zone, capturing variations in effect through intercept and slope adjustments as LCZ types change.

The fundamental equations are as follows: Eq. (4) serves as the null model, providing a constant baseline, while Eq. (5) outlines the basic linear model that includes only the independent variable and constant term. Eq. (6) expands this framework into a linear mixed regression model by integrating random effects.

$$Y_1 = \alpha_0 + \mu_{0j} + \varepsilon_{ij} \quad (4)$$

$$Y_2 = \alpha_0 + \beta_i * X_i + \mu_{0j} + \varepsilon_{ij} \quad (5)$$

$$Y_{ij} = (\alpha_0 + \beta_i \times X_i) + (\mu_{0j} + \mu_{1j} \times X_i + \varepsilon_{ij}) \quad (6)$$

Y_{ij} is the CEI for the i block of the j class LCZ zone, α_0 is the average level of carbon emissions across all samples (i.e., total model intercept), β_i is Fixed-effects coefficients on the effect of finger morphological indicators on CEI, X_i is the i block morphological indicators, ε_{ij} is the residual (referring to the difference in carbon emission levels between individual blocks), μ_{0j} is the intercept value of the effect of the j LCZ zone on block CEI, μ_{1j} is the random effect influence coefficient on the i morphological indicators within the j LCZ zone.

3. Results

3.1. Distributional characteristics of carbon emissions in blocks

The CEI across various residential blocks is presented in Fig. 6, with LCZ4-61 showing the lowest CEI and LCZ6-108 the highest. Table 6 provides a summary of the CEI ranges, average intensity values, and variations within each sample group. The ranking of average CEI is as follows: LCZ6>LCZ3>LCZ2>LCZ1>LCZ4> LCZ5. Generally, high-rise areas display lower CEI compared to low-rise open building zones. Additionally, by calculating the dispersion coefficient to analyze the fluctuations in CEI among different blocks, it is observed that the compact high-rise zone exhibits considerable fluctuation. In contrast, the compact mid-rise zone represents the urban morphology with the best carbon reduction and environmental performance stability, attributed to higher building density, smaller pore spaces between buildings, and reduced interference from external climatic conditions, which

stabilize heat gain and transfer processes within individual buildings. Conversely, high-rise zones facilitate wind development, leading to turbulent exchanges between cold and warm air, undermining local microclimate stability. Low-rise areas struggle to manage high energy consumption in their peripheral spaces, resulting in the most unstable carbon emissions in high-rise zones, while emissions per unit area in low-rise buildings are the highest.

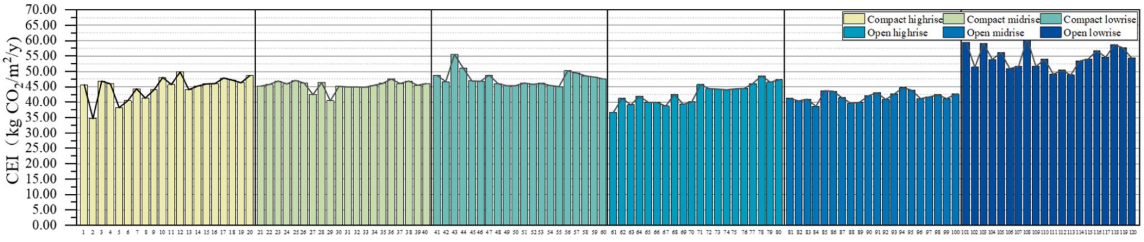

Fig. 6. Distribution characteristics of CEI in LCZ1-6

Table 6 Distribution level of block CEI in different LCZ zones

	LCZ1	LCZ2	LCZ3	LCZ4	LCZ5	LCZ6
STDEVP	3.5681	1.5586	2.4768	3.1881	1.5135	3.4397
CEI Range（kg $CO^2/m^2/y$）	34.65-49.80	40.40-47.44	45.02-55.50	36.69-48.52	38.58-44.68	48.77-60.52
AVERAGE（kg $CO^2/m^2/y$）	44.76	45.44	47.64	42.70	41.74	54.25
Dispersion Coefficient	0.0797	0.0343	0.0520	0.0747	0.0363	0.0634

3.2. Correlation analysis between morphological factors and carbon emissions

The CEI was utilized as the dependent variable, while various urban morphological indicators functioned as independent variables. A correlation analysis was conducted using Pearson's test, with a p-value confidence interval set at 95 %. The analysis revealed varying degrees of auto-correlation among factors such as FAR, BI, SVF, BER, FAI, and GSR. After a comprehensive comparison, BI, GSR, SVF and BER were excluded from further analysis and the subsequent regression model fitting process. H/W, L/W, FAR, BCR, and PO are negatively correlated with CEI, with significance levels above 0.01; whereas O, BSF, SVF, and FAI are positively correlated with CEI. The Building shape factor and CEI exhibited a strong correlation at the 0.01 level (0.81^{***}), thereby corroborating existing studies. (Fig. 7)

Further analysis of various regional samples reveals several key findings: (1) Overall, compact zones show a stronger correlation between morphological factors and CEI, whereas open zones frequently lack statistically significant correlations. Even considering variations in block sample sizes, it appears that the "urban morphology-carbon emission" relationship is more accurately captured in compact blocks, where three-dimensional morphological characteristics directly influence carbon emission levels; (2) Compared to block-layout indicators, the correlations between building-scale geometrical features and CEI are less variable in relation to

changes in LCZ types, showing stability in their positive or negative relationships. This indicates significant spatial heterogeneity in how building layout patterns affect carbon emissions across urban areas, while building-scale design indicators maintain consistent relationships regardless of the block's density. Nonetheless, further investigation into specific quantitative relationships is needed; (3) The four urban morphological indicators—H/W, BSF, FAR, BCR and SVF demonstrate the strongest correlations with CEI, aligning closely with findings from the comprehensive sample analysis(Table 7).

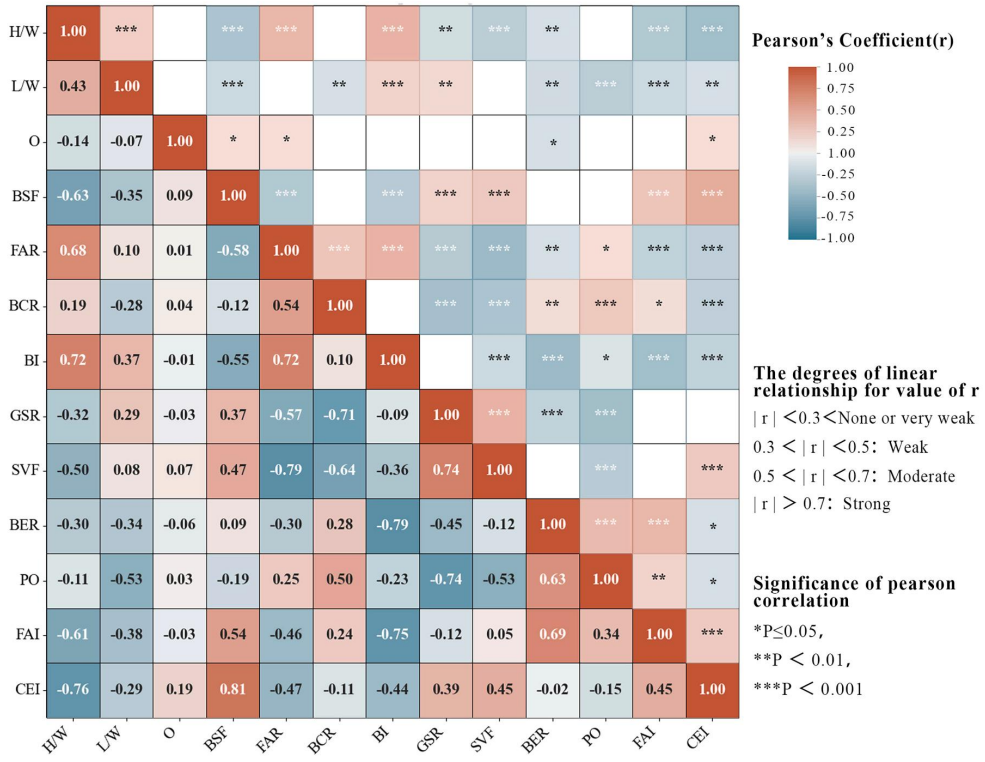

Fig. 7. The results of Pearson's correlation analysis.

Table 7 Correlation analysis of block urban morphological indicators and CEI in different LCZ zone

Morphological indicator	Compact High-rise	Compact mid-rise	Compact low-rise	Open High -rise	Open mid -rise	Open low -rise
H/W	-0.302***	-0.518***	-0.364**	-0.302**	-0.303**	-0.278**
L/W	-0.423	-0.455*	-0.187*	-0.215*	-0.206	-0.158
O	0.148	0.254*	0.247	0.450*	0.542**	0.610
BSF	0.627***	0.710***	0.452**	0.440**	0.127**	0.320**
FAR	0.557**	0.413**	-0.148***	-0.321**	0.343***	-0.231**
BCR	0.511**	0.365*	0.216**	0.167*	-0.221**	-0.279*
BI	-0.320**	-0.246*	0.198	-0.276	0.302	-0.165
GSR	-0.367	0.301	0.252	-0.264*	0.250**	0.301
SVF	0.461*	-0.343**	-0.290*	-0.372*	-0.292	-0.306
BER	0.243**	0.511*	0.603	-0.456	-0.107	0.225
PO	-0.174	0.408*	-0.411	0.301*	-0.414*	-0.543
FAI	0.315*	0.440**	-0.372*	-0.254**	-0.230**	0.106*

3.3. Estimation results by multilevel LMM

3.3.1. Relationship between the type of LCZ zones on carbon emissions

Fig. 8 presents scatter plots illustrating the relationship between morphological indicators and CEI, with linear regression curves fitted for different LCZ partitions and the entire sample, including confidence intervals for the latter. The sample point distribution revealed clustering in certain morphometric groups. Moreover, the intercept values and slopes of the regression curves across different LCZ zones and morphological groups varied significantly, indicating different varying underlying effects of LCZ types on CEI. These variations also interfered with the influence of urban morphology on CEI. Furthermore, the variation in the confidence region of the full-sample linear regression curve indicates heteroskedasticity in the model's error distribution and the differences in the relationship between samples and CEI across different LCZ zones. This illustrates that the LCZ effect, as the buildings environmental context, is significant in the model, although not all urban morphological factors respond to it.

The null model is established as a baseline, treating LCZ types as the primary variable while CEI serves as the dependent variable, without incorporating any morphological indicators as covariates. This approach requires the aggregation of CEI for each LCZ type during the operational phase and a covariance parameter estimation test. As shown in Table 8, the LCZ type significantly influences block carbon emissions, with an intercept term of 45.4155 that is statistically significant. The covariance parameter estimation results further indicate a stochastic effect associated with LCZ types. Table 9 includes both fixed effect and covariance parameter estimations for the null model, demonstrating that LCZ type accounts for 65.26 % of the variation in carbon emissions at the block level, as outlined in Eq. (7). The findings from the scatter plot and null model suggest initial evidence of spatial clustering in carbon emission performance among blocks within the same LCZ, where blocks exhibit similar CEI levels and are significantly different from those in other zones. This clustering could impact the relationship between urban morphological indicators and carbon emissions. After conducting the correlation analysis, fixed-effects models were fitted for urban morphological factors and carbon intensity at the block level, excluding the variables BER, BI, GSR, and SVF.

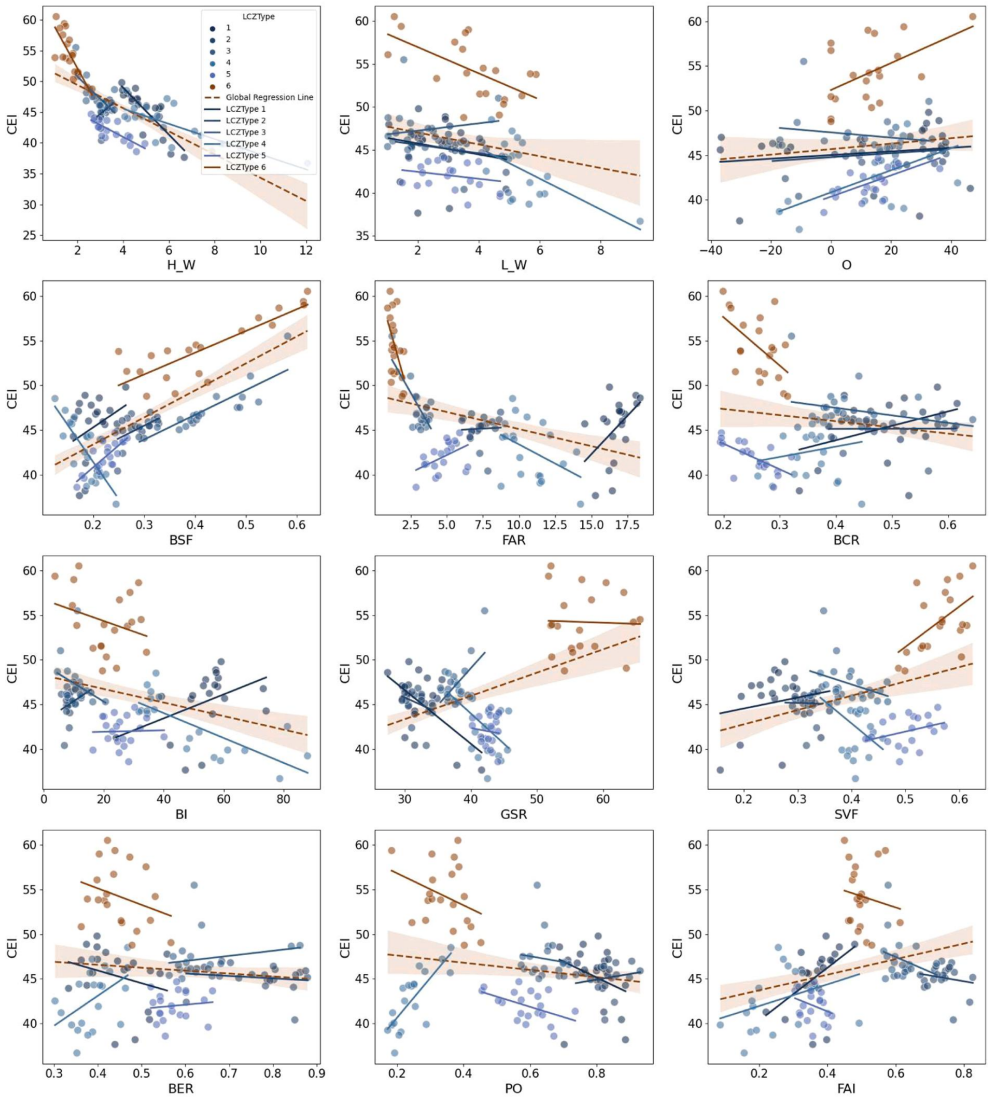

Fig. 8. Scatter plot of the relationship between morphological factors and CEI.

$$\rho = \frac{\sigma^2_{\mu 0 j}}{\sigma^2_{\mu_0 j} + \sigma^2_{\varepsilon_i j}} \quad (7)$$

ρ is the spatial aggregation of blocks CEI values, $\sigma^2_{\mu 0 j}$ ， is the intercept variance estimate， $\sigma^2_{\varepsilon_i j}$ is the residual estimate.

Table 8 The CEI null model's fixed effects estimation (without introducing morphological factors)

Fixed effects Estimation [a]							
Parameters	estimated value	standard error	degree of freedom	t	Significance	95% Confidence Intervals	
						lcl	ucl
Intercept	45.4155	1.8791	5	24.168	0.000	40.5850	50.2459

Table 9 The CEI null model's covariance parameters estimation

Covariance Parameters Estimation [a]					
Parameters	estimated value	standard error	Wald Z	Significance	95% Confidence Intervals

				level	lcl	ucl
Residual	9.0755	1.4003	6.481	0.000	6.7070	12.2804
Intercept[main=LCZ Type] variance	17.0508	10.1940	1.673	0.031	5.2825	55.0359

3.3.2. Fixed-effects of morphological factors on carbon emissions

Table 10 presents the estimated values of the fixed effects parameters, with the overall intercept of the model calculated at 50.8590. The factors of H/W, BSF, FAR, and FAI have produced the main contribution to the predicted value of the block's carbon emissions. The regression coefficients are − 1.3454, 8.8096, − 0.3683, and − 4.3643. The rank order of their contribution to carbon emissions is BSF > FAI > H/W > FAR. BSF has the greatest influence, i.e., for every unit change in BSF compared with H/W, its influence on the carbon emission value is 16.9 times that of the H/W change. The remaining morphological factors, while exhibiting a linear relationship with carbon emission values in a one-factor correlation analysis, do not demonstrate significant performance in the regression model. This indicates that when the effects of multiple factors are considered simultaneously, these parameters contribute significantly less to the dependent variable compared to the four aforementioned parameters.

Table 10 The fixed effects parameters estimation (introducing morphological indicators as covariant variable)

Fixed Effects Parameters Estimation [a]							
Parameters	Estimated value	standard error	degree of freedom	t	Significance	95% Confidence Intervals	
						lcl	ucl
intercept	50.859000	2.831299	78.206	17.963	0.000	45.222521	56.495421
H/W	-1.345484	0.411150	4.483	-3.272	0.000	-2.440104	-0.250865
L/W	-0.015154	0.217706	2.337	-0.070	0.154	-0.833649	0.803342
O	0.020178	0.009871	73.336	2.044	0.248	-0.000507	0.039850
BSF	8.809633	3.034151	74.471	7.518	0.000	16.764589	28.854677
FAR	-0.368342	0.086580	70.533	-2.518	0.001	-0.660048	-0.076636
BCR	-1.903400	5.019862	7.436	-0.379	0.715	-13.633794	9.826993
PO	-2.285046	3.330119	11.407	-0.686	0.506	-9.582794	5.012702
FAI	-4.364307	2.329926	59.450	-1.873	0.024	-9.025740	0.297126

a. dependent variable：CEI[kg $CO^2/m^2/y$]

3.3.3. Random-effects of morphological factors on carbon emissions

The model construction is based on LCZ type, integrating the main effects of all morphological factors during the random-effects estimation. A restricted maximum likelihood (REML) method is applied, along with covariance parameter estimates, to clarify the random effects of these factors. The results indicate significant responses

of H/W, BSF, FAR, BCR, and FAI to LCZ with random effects. Notably, BCR, previously deemed insignificant in the fixed-effects model, emerged as significant in the random-effects model and, like FAR, demonstrated a negative correlation. This suggests that increasing the building density of 2D structures contributes to favorable microclimate conditions, thereby reducing carbon emissions. The covariance estimates reflect valid regression coefficients for factors influenced by LCZ type (Table 11), showing that a one-unit change in these indicators adjusts the block's CEI accordingly. Table 12 highlights that including LCZ zoning increases the complexity of the relationship between morphological factors and CEI. When assessed using the information criterion, the model presents a smaller scale compared to both the null and fixed-effects models, suggesting that the CEI prediction model with both fixed and random effects offers a superior fit, affirming its scientific validity. Further investigation is needed to precisely quantify the distinct effects of various LCZ zones on morphological indicators, as their influence may be subtler than initially perceived.

Table 11 The LMM's covariance parameters estimation

Covariance Parameters Estimation [a]						
Parameters	Estimated value	standard error	Wald Z	Significance	95% Confidence Intervals	
					lcl	ucl
residuals	2.139080	0.441983	4.840	0.000	1.426755	3.207041
intercept	1.393274	25.30470	0.055	0.000	0.241250	5.464210
H/W	-0.614802	0.636912	0.965	0.000	0.080709	4.683258
L/W	-0.091650	0.255802	0.358	0.720	0.000386	21.77210
O	0.015226	0.004742	3.211	0.513	0.008270	0.028032
BSF	1.318900	1.402273	1.190	0.000	0.321500	8.662500
FAR	-1.802751	0.005189	2.457	0.001	0.005743	0.283110
BCR	-1.866600	1.563400	1.194	0.017	0.361495	9.638368
PO	-0.014743	0.004640	3.177	0.443	0.007956	0.273190
FAI	-0.891949	0.018766	4.900	0.061	0.061635	0.137174

a.dependent variable：CEI[kg $CO^2/m^2/y$]

Table 12 Information criterion test

Information criterion [a]			
	Null-model	Fixed-effect model	Random-effect model
-2 Restricted log-likelihood	284.019	243.105	216.575
Akaike information criterion (AIC)	288.019	247.105	220.575
AICC (Corrected Akaike Information Criterion)	288.292	247.413	220.882
CAIC (Consistent Akaike Information Criterion)	293.719	252.580	226.050
BIC (Bayesian Information Criterion)	291.719	250.580	224.050

Table 13 presents the fixed influence values of six LCZ zoning districts on block carbon emissions, showing figures of 2.310 kg $CO^2/m^2/y$, 0.908 kg $CO^2/m^2/y$, 1.256 kg $CO^2/m^2/y$, 1.551 kg $CO^2/m^2/y$, 1.519 kg $CO^2/m^2/y$, and 3.901 kg $CO^2/m^2/y$.

Compact zones generally exhibit a lower baseline impact on CEI compared to open zones, with LCZ6 having the highest and LCZ2 the lowest values. Furthermore, the sensitivity of morphological factors to microclimate responses tends to be significantly greater in compact building areas than in open spaces. The H/W and BSF indicators display relatively stable coefficient variations across different LCZ zones, likely due to their association with monolithic forms that reflect block proportionality rather than detailed geometric features of single building (e.g., length, width, height). The variations between sample zones are moderated, resulting in a consistent influence of these indicators on carbon emissions regardless of LCZ differences. For instance, a unit change in BSF affects CEI differently across LCZ zones: 1.310 kg $CO^2/m^2/y$, 1.710 kg $CO^2/m^2/y$, 1.468 kg $CO^2/m^2/y$, 1.502 kg $CO^2/m^2/y$, 1.461 kg $CO^2/m^2/y$, and 0.865 kg $CO^2/m^2/y$. In contrast, block buildings layout indicators like FAR and BCR show substantial sensitivity to LCZ zoning, with both the magnitude and the nature of their relationships with carbon emissions shifting across sample zones. As the LCZ type transitions from 1 to 6, the effects on CEI for FAR and BCR change from negative to positive values. They act synergistically, collectively reflecting the intensity of block construction in two- and three-dimensional contexts. The FAI, conversely, behaves oppositely to building intensity indicators.

Table 13 The random-effect coefficients for morphological factors introducing LCZ

Covariance Parameters Estimation [a]						
Parameters	Compact High-rise	Compact mid-rise	Compact low-rise	Open High -rise	Open mid -rise	Open low -rise
Residual (kg $CO^2/m^2/y$)	2.670	3.021	0.763	-0.573	0.056	0.314
Intercept (kg $CO^2/m^2/y$)	2.310	0.908	1.256	1.551	1.519	3.901
H/W	-0.412***	-0.463***	-0.510***	-0.519**	-0.496**	-0.512**
L/W	0.680*	0.586	0.673**	0.710	0.761*	0.604*
O	0.389*	0.641	0.430*	1.121**	1.057	1.352
BSF	1.310***	1.710**	1.468***	1.502**	1.461**	0.865***
FAR	1.565**	0.670***	-0.245***	-1.422***	-1.419***	-.550**
BCR	1.030***	0.562**	0.242**	-0.651***	-0.823**	-1.078**
PO	-0.215*	-0.126*	-0.431	-0.379	-0.325*	-0.404*
FAI	-0.402*	-0.253***	-0.217**	0.403*	0.241*	0.133**

The Color labels indicate coefficient size and significance

These analyses yield the fixed and random impact coefficients for morphological factors affecting carbon emissions across the six LCZ zones. Moreover, corrections to the traditional multiple linear regression model resulted in six new predictive models that better represent the interactions between building morphology and urban climate conditions (Fig. 9).

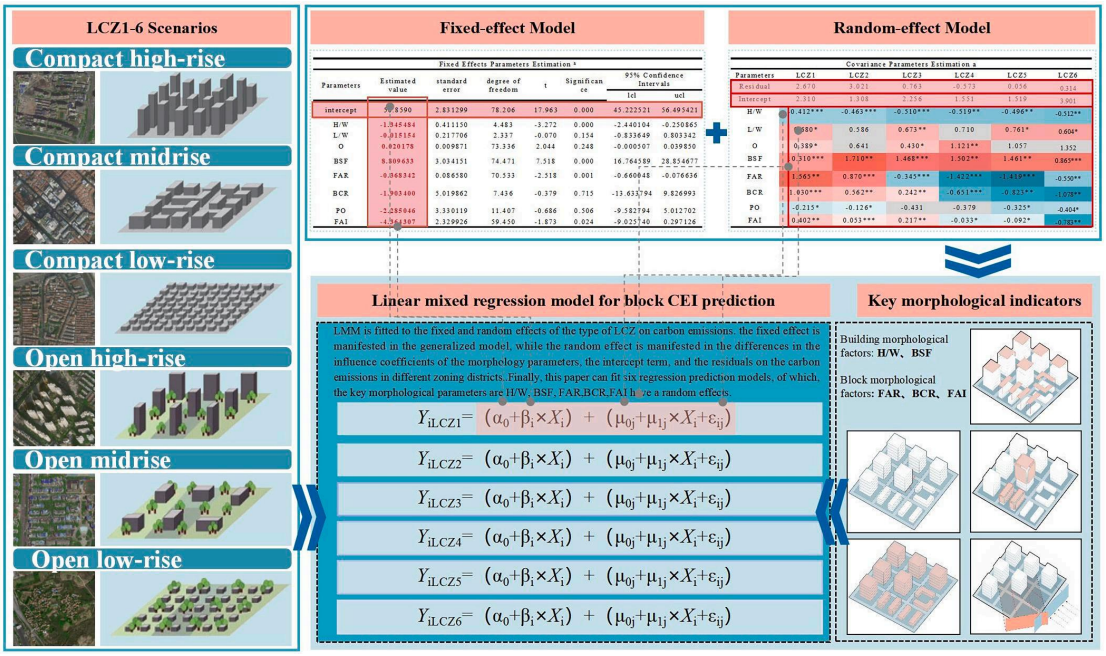

Fig. 9. Linear mixed-effect regression model for CEI introducing LCZ.

4. Discussion

4.1. The rationality of the application of LMM

The LMM outperforms traditional ordinary least squares model and generalized linear model in analyzing hierarchical panel data, effectively capturing both correlations and non-synchronicity. Unlike standard linear regression, which primarily focuses on averages, LMM accounts for variance structures that represent inter- and intra-group variability. This makes it particularly well-suited for exploring complex relationships among diverse groups. Previous research on urban morphology's impact on building energy use has often utilized similar methodologies to analyze hierarchical data and compare group differences. However, many of these studies either examine each group in isolation or rely on basic statistical descriptions, failing to investigate internal relationships and interactions comprehensively (Ahmadian et al., 2021; Xie et al., 2023). While such approaches highlight group effects on variable coefficients, they often overlook the nuanced insights that LMM can provide. By integrating both fixed and random effects, LMM captures the overall influence of variables alongside specific impacts at the group level, offering a more holistic perspective. In contrast, grouped regression models treat each group independently, which can limit information exchange and lead to underestimated standard errors or misleading conclusions. Thus, LMM is more appropriate for this study, and its effectiveness has been validated across various fields in urban science research (Xin & Feng, 2024; Qian et al., 2023).

It is also noteworthy that this study does not utilize complex machine learning models or AI-driven data analysis techniques. This decision was based on both the small sample size and the desire to maintain model interpretability and the influence of individual variables. While machine learning can enhance predictive accuracy and model nonlinear relationships, it often results in "black-box" models that may not be suitable for every research objectives.

4.2. Relationship between the morphological factors, LCZ type and carbon emissions

This study finding indicate that the urban context defined by the LCZ not only directly influences block carbon emission levels but also further impacts how urban block morphological factors affect carbon emissions.

4.2.1. Direct effect of LCZ on block carbon emissions

The null model results reveal significant spatial heterogeneity among different LCZs used for classifying urban blocks. Notably, variations in LCZ types explain 65.26 % of the changes in carbon intensity levels within residential blocks, highlighting pronounced spatial clustering and differences due to geographic location and urban morphology. Within each LCZ, similarities in the built environment—including surface temperature, ground cover, wind speed, humidity, and precipitation—are evident (Cai et al., 2023). The mean carbon intensity values for the other two types of open blocks differ by less than 1 kg $CO^2/m^2/y$, marking the lowest among all types. The overall intensity value for compact blocks is moderate. Taking into account the standard deviation and coefficient of variation in CEI, the residential blocks in the compact mid-rise zone exhibit the least variation in CEI values. Although they do not have the lowest CEI, they show the most stable pattern of variation, compared to the open high-rise and mid-rise zones, which exhibit lower carbon intensity levels but experience substantial variation between individual samples. This suggests that small changes in block morphology or microclimate conditions are likely to introduce unpredictable fluctuations in carbon emission levels.

The compact urban layout, with higher building envelopes and lower porosity, reduces microclimate disturbances and heat flow on building surfaces, stabilizing residents' energy consumption patterns. In addition, numerous other relevant studies have reported that compact LCZ types exhibit significantly higher building-level solar PV potential (Chen et al., 2024). Considering all factors, LCZ2 emerges as one of the most influential and adaptable urban forms for reducing carbon emissions within the study area. Comparing to the LCZ1 and 3, LCZ2 remains the most densely populated

blocks type. In Wuhan, these zones are predominantly located in older urban areas, where commercial activity and residential density peak, further emphasizing the importance of solar photovoltaic (PV) technology, as one of the most commonly used clean energy technologies, in promoting its application in old urban areas to create low-carbon communities and expand environmental benefits. However, poor design may disrupt ventilation and solar exposure, intensifying the heat island effect, thereby increasing building energy use and carbon emissions (Xu et al., 2021), which will need to be further discussed in conjunction with further analysis of the effects of urban morphological variables. The high CEI of LCZ6 offers valuable insights for planning low-density residential areas, such as villa zones. These areas are often situated in peri-urban zones, where they are more susceptible to climatic variability. As such, centralized planning layouts should be considered to minimize fluctuations in residential energy use.

4.2.2. Inherent effects of morphological factors on block carbon emissions

The regression coefficients from the fixed-effects model illustrate the inherent relationship between morphological indicators and CEI without the influence of specific urban contexts, offering designers clear guidance for their decisions. In terms of building scale, an increase of one unit in the building shape factor leads to a rise in CEI of 8.8096 kg $CO^2/m^2/y$, the highest among the morphological indicators, aligning with findings from other studies (Qi et al., 2019). BSF reflects the external surface area for heat loss; a larger area results in increased energy loss for the same building volume (Baglivo et al., 2024). For residential structures, the shape, equipment room placement, household layout, and number of balconies influence this external surface's concavity and convexity. The H/W is another critical morphological factor affecting carbon emissions, showing a negative correlation with CEI. Specifically, each unit decrease in this ratio results in a reduction of 1.3458 kg $CO^2/m^2/y$ in CEI. As the average height of building units increases and their width decreases, the block's overall form approaches that of LCZ4 and LCZ5, which research indicates correlates with lower carbon emissions. Regarding block-scale layout indicators, the FAR negatively correlates with block CEI (Huang & Niu, 2016). Within specific limits, a higher FAR suggests a denser urban structure, supporting findings related to the impact of LCZ on CEI. This reinforces the compact development model advocated by sustainable urban principles. Additionally, the FAI also negatively influences CEI; a larger FAI reduces mutual shading among buildings, enhancing air circulation and mitigating the heat island effect. This is particularly relevant in Wuhan, where the demand for air conditioning constitutes a significant portion of annual

energy consumption. Consequently, increasing FAI can effectively lower the district's carbon emissions.

4.2.3. Indirect effect of LCZ on block carbon emissions

The indirect influence of LCZ is primarily reflected in how block urban morphological indicators affect carbon emissions, resulting in additional impacts. This relationship is articulated through intercept and coefficient estimates derived from the final cluster random effects model. The intercept values of the grouped random effects model reveal the baseline impacts of various LCZ types on the CEI of their respective residential blocks, as detailed in the RESULTS section. Notably, LCZ2 exhibits the lowest baseline impact on CEI, reaffirming its status as a desirable urban block pattern with low carbon potential. The slopes in the model indicate the sensitivity of morphological factors to microclimate variations. Compact areas significantly influence these factors, emphasizing the importance of controlling block morphology in densely built environments, such as city centers, when planning low-carbon communities. Enhancing the shape of buildings and layout in these areas is likely to yield greater carbon reduction benefits compared to less dense regions, making it a more manageable approach than optimizing energy sources or electrical systems. Not all factors show random effects on CEI. Significant coefficients suggest that H/W, BSF, FAR, BCR, and FAI are influenced by LCZ, albeit to different extents. Planners should prioritize these factors to improve the climate adaptability of block designs. Overall, the introduction of LCZs indicates a non-linear relationship between block layout indicators and carbon emissions.

The findings further illustrate how the impacts of these morphological factors vary across different LCZs. Urban layout indicators are more responsive to block compactness than single-building geometry, which exhibits consistent regression coefficients. Building-scale morphological indicators like H/W maintain impact coefficients around -0.480, while BSF stabilizes around 1.50. This is the same as the fixed-effects model, which remains one of the most effective form indicators for carbon emissions. The impact effects on building layout indicators validates similar conclusions in some previous related research advances. Ewing et al. found that there is a "U" shaped relationship between building density and energy consumption (Ewing & Rong, 2008), while the study by Javadpoor et al. found an inverse "U" shaped relationship between them, which is consistent with the nonlinear character of the relationship found in this study (Javadpoor et al., 2024). As discussed in Section 4.2.2, building density must be moderated; excessively high density can adversely affect energy consumption and carbon emissions, particularly in residential areas with

higher activity levels. Thus, an appropriate level of "development intensity" is beneficial for low-carbon blocks. However, for different cities, targeted studies are needed to determine a reasonable range of adjustment of morphological indicators, which also further demonstrates the value of this study for the development of low-carbon blocks in Wuhan. The FAI has an opposite effect to that of the building intensity index, with a positive "U" shaped relationship as the building intensity decreases, and as the block becomes more open, the increase in the facade area ratio may lead to more wind pressure, cooling effects, and more heat loss from the exterior surfaces of the building, especially in colder climates conditions. This may lead to more building energy consumption and carbon emissions. The linear impact of building scale design indicators and the non-linear impact of block building layout indicators illustrate the need to consider the impact of the geographic location of the block, the particular built environment, and the synergistic relationship between these indicators and individual building design indicators (e.g., building shape factors) when designing the urban form of a low-carbon block to maximize the overall low-carbon effectiveness.

4.3. LCZ-based zoning method for low-carbon city planning

The concept of "zoning" was introduced to facilitate more systematic and efficient urban development. Traditional zoning primarily focuses on aesthetic and functional goals, yet, despite growing concern for climate impacts, standard zoning methods often fail to address the interactions between climate conditions and spatial design during the urban planning phase. While building-density-based zoning is common in urban science research, it lacks universally accepted definitions, limiting its practical use. Similarly, land-use zoning, which categorizes areas by activities, frequently neglects low-carbon performance metrics. These conventional planning approaches do not adequately address the complexities of urban climates, and several factors—including economic constraints, reliability of meteorological data, evaluations of urbanization policies, and gaps in foundational knowledge—hinder the implementation of climate-resilient planning (Handley & Carter, 2006; Luo et al., 2019).

LCZ serve as a zoning method that illustrates the connection between urban morphology and microclimates, making it an effective framework for climate-adaptive planning. Previous work, such as Wu' s study utilized big data analysis within the LCZ framework to evaluate carbon emissions across different urban zones (Wu et al., 2018). While this approach mapped emissions at an urban scale, it also identified limitations in LCZ's ability to capture the energy

characteristics and CEI of various urban zones. Notable limitations include understanding the specific impact pathways of urban morphology within different LCZs, energy consumption behaviors of diverse functional buildings, and other dynamic factors like traffic patterns that design cannot easily control. Future research and practical applications must consider these elements. The current LCZ method requires further refinement, with the development of new conceptual models such as "Local Energy Zones" (LEZ) or "Local Carbon Zones". The concept of LEZ, proposed by Sharifi et al. (Wu was also a co-author in the study), is based on the LCZ framework but integrates measurable urban morphological variables, urban blocks' layout characteristics, and select socioeconomic indicators like population density and economic levels. LEZ is expected to establish a more effective framework for assessing and mapping carbon emissions while inheriting LCZ's core spatial and morphological attributes (Sharifi et al., 2018). Although LCZ faces challenges in practical application, it remains a valuable source of inspiration. And some other researchers have begun to try to apply this LCZ-based mapping model to other cities to test the generalizability of this working framework (Javadpoor et al., 2024).

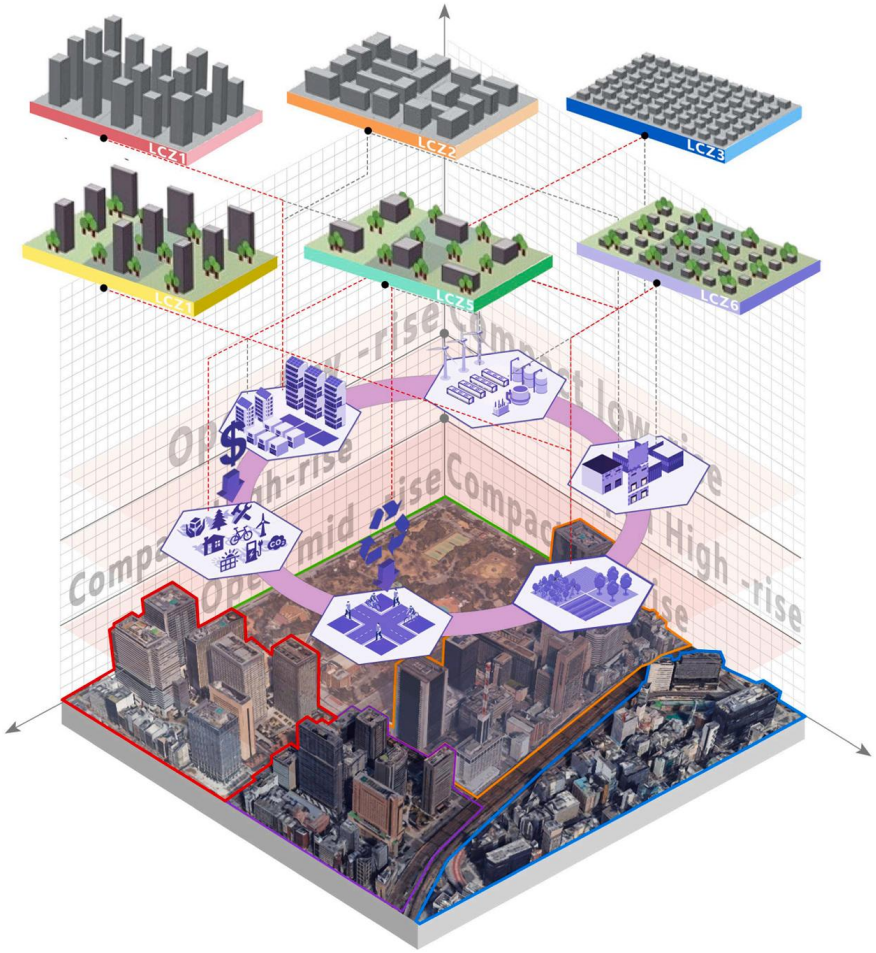

Fig. 10. Low-carbon urban management strategy based on the LCZ framework.

This study enhances the understanding of the relationship between LCZ and urban building energy use, emphasizing the potential for realizing the integration of urban climate research with urban planning and design efforts at the neighborhood level, compared to existing studies (Chen et al., 2021; Guerra et al., 2023; Jiang et al., 2023; Khamchiangta & Yamagata, 2024; Liu et al., 2018; Yang et al., 2020). Although it does not fully resolve previous limitations, this research adopts a bottom-up approach to measure carbon emissions at the urban block level. Additional block-level morphological features were introduced as covariates to elucidate the mechanisms behind the carbon emission map and the variations in emission levels across different zones. By analyzing the regression coefficients from the carbon emission model, we propose optimization methods for urban morphology and design strategies to manage emissions across zones, addressing differences in the impact of urban morphology within LCZs. This study identifies five key morphological characteristics—height-to-width ratio, shape coefficient, floor area ratio, building coverage density, and windward building surface area ratio—that correlate with both LCZ type and carbon emissions. However, the complexity of these relationships extends beyond these factors. Expanding this methodology to cover larger areas and additional cities could lead to a comprehensive regulatory system for morphological indicators, facilitating precise adjustments to building energy demand and other carbon-emitting activities. This research can also be broadened to develop carbon emission maps for various regions using standardized metrics, as well as low-carbon design guidelines and management strategies for specific zones, ultimately supporting the transformation of LCZs into a standardized measurement framework for “Local Carbon Zones” (Fig. 10).

4.4. Limitations and future research

Only residential blocks were chosen for energy simulations in this study, even though LCZ zones typically include a variety of building types. Future studies should consider the carbon emissions of all buildings within each sample area, and additional influential factors, such as motorized traffic and green space, should be incorporated, which is likewise a shortcoming in the Wu et al. study. Additionally, the carbon emissions per unit area of buildings over the entire year are selected as the dependent variable in this study, which eliminates the influence of temporal factors, thereby facilitating comparative analysis. Nevertheless, the morphology of different LCZs varies significantly, which could further complicate the effects of morphological factors on building energy consumption and carbon emissions across various seasons

and time periods. Therefore, future research needs to comprehensively consider both temporal and spatial effects to refine the current conclusions.

5. Conclusions

This study reevaluates the relationship among local urban climatic conditions, block morphology, and carbon emissions, which contribute to the construction of a standardized "urban form-carbon emission" spatial unit mapping model. It identifies the direct and indirect effects of LCZs on carbon emissions in residential blocks and determines the most suitable LCZ types for developing low-carbon blocks. Additionally, the study proposes low-carbon urban form design strategies tailored to specific LCZ zones, based on quantitative regression coefficients that assess the influence of urban form variables on carbon emission levels.

These findings provide valuable insights for developing urban energy policies, as well as for the planning and design of urban blocks. Future urban planners and government officials can leverage the LCZ zoning method and the experimental concepts presented here to refine zoning management practices, improving the connection between carbon emissions and urban morphology. However, to better assess the generalizability of the LCZ framework as a contextual basis for measuring carbon emissions and building energy use across cities, further research is needed in different regions. This should include comparisons with traditional zoning scenarios to evaluate the applicability of both approaches.

Funding

The work described in this paper was Funded by the National Natural Science Foundation of China (NSFC NO. 52378020); Open Foundation of the State Key Laboratory of Subtropical Building and Urban Science (NO. 2023KA02); Program for HUST Academic Frontier Youth Team (No. 2019QYTD10).

CRediT authorship contribution statement

Yuchen Qin: Writing — original draft, Visualization, Methodology, Formal analysis, Data curation, Conceptualization. Jian Kang: Writing—review & editing, Supervision. Haizhu Zhou: Resources, Methodology, Conceptualization. Shen Xu: Resources, Project administration, Methodology, Funding acquisition, Conceptualization. Gaomei Li: Writing–review & editing, Software, Methodology. Chenqi Li: Writing—review & editing, Software, Methodology. Wenjun Tan: Writing —review & editing, Software.

Declaration of competing interest

The authors declare that they have no known competing financial interests or personal relationships that could have appeared to influence the work reported in this paper.

Data availability

The authors do not have permission to share data.

References

Adolphe, L. (2001). A simplified model of urban morphology: Application to an analysis of the environmental performance of cities. Environment and Planning B: Planning and Design, 28(2), 183–200.

Ahmadian, E., Sodagar, B., Bingham, C., Elnokaly, A., & Mills, G. (2021). Effect of urban built form and density on building energy performance in temperate climates. Energy and Buildings, 236, Article 110762.

Ahn, Y., & Sohn, D. W. (2019). The effect of neighbourhood-level urban form on residential building energy use: A GIS-based model using building energy benchmarking data in Seattle. Energy and Buildings, 196, 124–133.

Ali-Toudert, F., & Mayer, H. (2006). Numerical study on the effects of aspect ratio and orientation of an urban street canyon on outdoor thermal comfort in hot and dry climate. Building and Environment, 41(2), 94–108.

Allan, J., Eggimann, S., Wagner, M., Ho, Y. N., Züger, M., Schneider, U., & Orehounig, K. (2022). Operational and embodied emissions associated with urban neighbourhood densification strategies. Energy and buildings, 276, Article 112482.

Anderson, J. E., Wulfhorst, G., & Lang, W. (2015). Energy analysis of the built environment—A review and outlook. Renewable and Sustainable Energy Reviews, 44, 149–158.

Ao, Y., Yang, D., Chen, C., & Wang, Y. (2022). Effects of the built environment on travelrelated CO2 emissions considering travel purpose: A case study of resettlement neighborhoods in Nanjing. Buildings, 12(10), 1718.

Baglivo, C., Albanese, P., & Congedo, P. (2024). Relationship between shape and energy performance of buildings under long-term climate change. Journal of Building Engineering, 84, Article 108544.

Banerjee, S., Pek, R. X. Y., Yik, S. K., Ching, G. N., Ho, X. T., Dzyuban, Y., … Chow, W. T. L. (2024). Assessing impact of urban densification on outdoor microclimate and thermal comfort using ENVI-met simulations for Combined

Spatial-Climatic Design (CSCD) approach. Sustainable Cities and Society, 105, Article 105302.

Barone, F., Merlier, L., Bouquerel, M., & Kuzonik, F. (2024). Heat stress assessment using an urban microclimate zonal model at the block scale coupled with building models. Sustainable Cities and Society, Article 106009.

Bonenberg, W., Skorzewski, W., Qi, L., Han, Y., Czekala, W., & Zhou, M. (2023). An energy-saving-oriented approach to urban design—Application in the local conditions of Poznan´ metropolitan area (Poland). Sustainability, 15(14), 10994.

Cai, M., Ren, C., Shi, Y., Chen, G., Xie, J., & Ng, E. (2023). Modeling spatiotemporal carbon emissions for two mega-urban regions in China using urban form and panel data analysis. Science of the Total Environment, 857, Article 159612.

Cang, Y., Yang, L., Luo, Z., & Zhang, N. (2020). Prediction of embodied carbon emissions from residential buildings with different structural forms. Sustainable Cities and Society, 54, Article 101946.

Chatterjee, S., & Dinda, A. (2022). Determination of characterized urban thermal zones (UTZ) for assessing microclimates in the tropical metropolitan area of Kolkata. Sustainable Cities and Society, 80, Article 103807.

Chen, X., Tu, W., Yu, J., Cao, R., Yi, S., & Li, Q. (2024). LCZ-based city-wide solar radiation potential analysis by coupling physical modeling, machine learning, and 3D buildings. Computers, Environment and Urban Systems, 113, Article 102176.

Chen, X., Yang, J., Ren, C., Jeong, S.j., & Shi, Y. (2021). Standardizing thermal contrast among local climate zones at a continental scale: Implications for cool neighborhoods. Building and Environment, 197, Article 107878.

Cui, P., Lu, J., Wu, Y., Tang, J., & Jiang, J. (2024). Effect of urban morphology on microclimate and building cluster energy consumption in cold regions of China. Sustainable Cities and Society, Article 105838.

Deng, J., Wong, N., & Zheng, X. (2016). The study of the effects of building arrangement on microclimate and energy demand of CBD in Nanjing, China. Procedia Engineering, 169, 44–54.

Dong, Q., Huang, Z., Zhou, X., Guo, Y., Scheuer, B., & Liu, Y. (2023). How building and street morphology affect CO2 emissions: Evidence from a spatially varying relationship analysis in Beijing. Building and Environment, 236, Article 110258.

Du, S., Kuang, X., Chen, J., Ye, Y., Li, P., & Shi, X. (2024). Development of an expanded local climate zone scheme to accommodate diversified urban morphological evolution: A case study of Shanghai, China. Urban Climate, 56, Article 102009.

Ewing, R., & Rong, F. (2008). The impact of urban form on US residential energy use. Housing policy debate, 19(1), 1–30.

Fang, C., Wang, S., & Li, G. (2015). Changing urban forms and carbon dioxide emissions in China: A case study of 30 provincial capital cities. Applied energy, 158, 519–531.

Fang, Y., Lu, X., & Li, H. (2021). A random forest-based model for the prediction of construction-stage carbon emissions at the early design stage. Journal of Cleaner Production, 328, Article 129657.

Fleischmann, M., Romice, O., & Porta, S. (2021). Measuring urban form: Overcoming terminological inconsistencies for a quantitative and comprehensive morphologic analysis of cities. Environment and Planning B: Urban Analytics and City Science, 48(8), 2133–2150.

Gamba, P., Lisini, G., & Lin, H. (2012). Urban climate zone detection and discrimination using object–based analysis of VHR scenes. Proceedings of the 4th GEOBIA, Rio de Janeiro,Brazil, 79(09), 56–70.

GBT 51366-2019. (2019). Ministry of Housing and Urban-Rural Development, PRC. Standard for Calculation of Building Carbon Emissions. Beijing, China: China Architecture & Building Press.

Gobakis, K., & Kolokotsa, D. (2017). Coupling building energy simulation software with microclimatic simulation for the evaluation of the impact of urban outdoor conditions on the energy consumption and indoor environmental quality. Energy and Buildings, 157, 101–115.

Guerra, P. S., Trigo, O. P., Espinosa, P. S., Cabrera, T. C., & Meseguer-Ruiz, O. (2023). Climate-sensitive planning. Opportunities through the study of LCZs in Chile. Building and Environment, 242, Article 110444.

Guo, Z., Wang, X., Luo, X., Zhao, N., & Wang, Q. (2024). Study on the influencing factors of carbon emissions of green public buildingsin the whole life cycle: A case study in hot summer and cold winter region. Building Science, 40(02), 12-18+29.

Handley, J., & Carter, J. (2006). Adaptation strategies for climate change in the urban environment. ASCCUE Draft final report to the National Steering Group. Centre for Urban and Regional Ecology, University of Manchester, Manchester.

He, P., Xue, J., Shen, G., Ni, M., Wang, S., Wang, H., & Huang, L. (2023). The impact of neighborhood layout heterogeneity on carbon emissions in high-density urban areas: A case study of new development areas in Hong Kong. Energy and Buildings, 287, Article 113002.

Huang, Y., Liu, J., & Ching, J. (2018). Research progress of WUDAPT project: Crowdsourcing solutions based on urban form, function information and its applications. South Architecture, (04), 26–33.

Huang, Y., & Niu, J. (2016). Optimal building envelope design based on simulated performance: History, current status and new potentials. Energy and Buildings, 117, 387–398.

Javadpoor, M., Sharifi, A., & Gurney, K. R. (2024). Mapping the relationship between urban form and CO2 emissions in three US cities using the local climate zones (LCZ) framework. Journal of Environmental Management, 370, Article 122723.

Ji, Q., Li, C., Makvandi, M., & Zhou, X. (2022). Impacts of urban form on integrated energy demands of buildings and transport at the community level: A comparison and analysis from an empirical study. Sustainable Cities and Society, 79, Article 103680.

Jiang, R., Xie, C., Man, Z., Afshari, A., & Che, S. (2023). LCZ method is more effective than traditional LUCC method in interpreting the relationship between urban landscape and atmospheric particles. Science of The Total Environment, 869, Article 161677.

Jiang, Y., Long, Y., Liu, Q., Dowaki, K., & Ihara, T. (2020). Carbon emission quantification and decarbonization policy exploration for the household sectorEvidence from 51 Japanese cities. Energy Policy, 140, Article 111438.

Kamal, A., Abidi, S. M. H., Mahfouz, A., Kadam, S., Rahman, A., Hassan, I. G., & Wang, L. L. (2021). Impact of urban morphology on urban microclimate and building energy loads. Energy and Buildings, 253, Article 111499.

Kamazani, M. A., & Dixit, M. K. (2023). Multi-objective optimization of embodied and operational energy and carbon emission of a building envelope. Journal of Cleaner Production, 428, Article 139510.

Khamchiangta, D., & Yamagata, Y. (2024). Mapping urban carbon emissions in relation to local climate zones: Case of the building sector in Bangkok Metropolitan Administration, Thailand. Energy and Built Environment, 5(3), 337–347.

Lan, T., Shao, G., Xu, Z., Tang, L., & Dong, H. (2023). Considerable role of urban functional form in low-carbon city development. Journal of Cleaner Production, 392, Article 136256.

Lee, J., Kurisu, K., An, K., & Hanaki, K. (2015). Development of the compact city index and its application to Japanese cities. Urban Studies, 52(6), 1054–1070.

Leng, H., Chen, X., & Ma, Y. (2020). Research progress on the lnfluence of urban form on building energy consumption and its enlightenments. Architectural Journal, (02), 120–126.

Li, N., & Quan, S. J. (2024). Discovering urban block typologies in Seoul: Combining planning knowledge and unsupervised machine learning. Cities, 150, Article 104988.

Li, Q., Xu, G., & Gu, Z. (2024). A novel framework for multi-city building energy simulation: Coupling urban microclimate and energy dynamics at high spatiotemporal resolutions. Sustainable Cities and Society, 113, Article 105718.

Li, R., Luo, L., Li, X., Wu, J., Jiang, F., & Wang, W. (2024). Multi-objective optimization for generative morphological design using energy and comfort models with a practical design of new rural community in China. Energy and Buildings, 313, Article 114282.

Lin, J., Lu, S., He, X., & Wang, F. (2021). Analyzing the impact of three-dimensional building structure on CO2 emissions based on random forest regression. Energy, 236, Article 121502.

Liu, K., Xu, X., Wang, W., & Zhang, R. (2023). A review of the research on the relationship between urban form and building energy consumption in the past 30 years. Architectural Journal, (S1), 120–127.

Liu, K., Xu, X., Zhang, R., Kong, L., Wang, W., & Deng, W. (2023). Impact of urban form on building energy consumption and solar energy potential: A case study of residential blocks in Jianhu, China. Energy and Buildings, 280, Article 112727.

Liu, L., Lin, Y., Xiao, Y., Xue, P., Shi, L., Chen, X., & Liu, J. (2018). Quantitative effects of urban spatial characteristics on outdoor thermal comfort based on the LCZ scheme. Building and Environment, 143(OCT), 443–460.

Liu, L., Zheng, B., & Bedra, K. (2018). Quantitative analysis of carbon emissions for new town planning based on the system dynamics approach. Sustainable Cities and Society, 42, 538–546.

Liu, X., & Sweeney, J. (2012). Modelling the impact of urban form on household energy demand and related CO2 emissions in the Greater Dublin Region. Energy Policy, 46, 359–369.

Liu, X., Wang, M., Qiang, W., Wu, K., & Wang, X. (2020). Urban form, shrinking cities, and residential carbon emissions: Evidence from Chinese city-regions. Applied Energy, 261, Article 114409.

Liu, Z., Cheng, W., Jim, C. Y., Morakinyo, T. E., Shi, Y., & Ng, E. (2021). Heat mitigation benefits of urban green and blue infrastructures: A systematic review of

modeling techniques, validation and scenario simulation in ENVI-met V4. Building and Environment, 200, Article 107939.

Liu, Z., Hu, Y., Qiu, Z., & Ren, F. (2024). Characteristics and prediction of traffic-related PMs and CO2 at the urban neighborhood scale. Atmospheric Pollution Research, 15(2), Article 101985.

Lombardi, M., Laiola, E., Tricase, C., & Rana, R. (2017). Assessing the urban carbon footprint: An overview. Environmental Impact Assessment Review, 66, 43–52.

Luo, X., Yu, C., Zhou, D., & Gu, Z. (2019). Challenges and adaptation to urban climate change in China: a viewpoint of urban climate and urban planning. Indoor and Built Environment, 28(9), 1157–1161.

Ma, J., Liu, Z., & Chai, Y. (2015). The impact of urban form on CO2 emission from work and non-work trips: The case of Beijing, China. Habitat Interbational, 47, 1–10.

Ma, X., Leung, T., Chau, C., & Yung, E. (2022). Analyzing the influence of urban morphological features on pedestrian thermal comfort. Urban Climate, 44, Article 101192.

Mao, X., Wang, L., Li, J., Quan, X., & Wu, T. (2019). Comparison of regression models for estimation of carbon emissions during building's lifecycle using designing factors: a case study of residential buildings in Tianjin, China. Energy and Buildings, 204, Article 109519.

Martin, L., & March, L. (1972). Urban Space and Structure. UK: Cambridge Press.

Mouzourides, P., Eleftheriou, A., Kyprianou, A., Ching, J., & Neophytou, M. K. A. (2019). Linking local-climate-zones mapping to multi-resolution-analysis to deduce associative relations at intra-urban scales through an example of Metropolitan London. Urban Climate, 30, Article 100505.

Mutschler, R., Rüdisüli, M., Heer, P., & Eggimann, S. (2021). Benchmarking cooling and heating energy demands considering climate change, population growth and cooling device uptake. Applied Energy, 288, Article 116636.

Natanian, J., & Wortmann, T. (2021). Simplified evaluation metrics for generative energy-driven urban design: A morphological study of residential blocks in Tel Aviv. Energy and Buildings, 240, Article 110916.

National Development and Reform Commission. (2011). Guidelines for the Preparation of Provincial GHG Inventories (for Trial Implementation); National Development and Reform Commission. Beijing, China: PRC.

Oliveira, V. M. A. (2022). Urban morphology. Springer International Publishing.

Parvar, Z., Mohammadzadeh, M., & Saeidi, S. (2024). LCZ framework and landscape metrics: Exploration of urban and peri-urban thermal environment emphasizing 2/3D characteristics. Building and Environment, 254, Article 111370.

Pasandi, L., Qian, Z., Woo, W. L., & Palacin, R. (2024). A comprehensive review of applications and feedback impact of microclimate on building operation and energy. Building and Environment, Article 111855.

Peng, F., Cao, Y., Sun, X., & Zou, B. (2024). Study on the contributions of 2D and 3D urban morphologies to the thermal environment under local climate zones. Building and Environment, 263, Article 111883.

Qi, F., Cui, F., Lv, W., Zhang, T., & Musonda, B. M. (2019). Regional similarity of shape coefficient of rural residences—Taking Hangzhou rural region as a case. Building Simulation, 12, 597–604.

Qian, J., Meng, Q., Zhang, L., Schlink, U., Hu, X., & Gao, J. (2023). Characteristics of anthropogenic heat with different modeling ideas and its driving effect on urban heat islands in seven typical Chinese cities. The Science of the Total Environment, 886, Article 163989.

Quan, S. J., Economou, A., Grasl, T., & Yang, P. P.-J. (2020). An exploration of the relationship between density and building energy performance. Urban Design International, 25, 92–112.

Quan, S. J., & Li, C. (2021). Urban form and building energy use: A systematic review of measures, mechanisms, and methodologies. Renewable and Sustainable Energy Reviews, 139, Article 110662.

Rock, M., Balouktsi, M., Saade, M. R. M., Rasmussen, F. N., Hoxha, E., Birgisdottir, H., … Lützkendorf, T. (2020). Embodied GHG emissions of buildings–Critical reflection of benchmark comparison and in-depth analysis of drivers. In IOP Conference Series. Earth and Environmental Science, 588, Article 032048.

Rostami, E., Nasrollahi, N., & Khodakarami, J. (2024). A comprehensive study of how urban morphological parameters impact the solar potential, energy consumption and daylight autonomy in canyons and buildings. Energy and Buildings, 305, Article 113904.

Sharifi, A. (2019). Resilient urban forms: A macro-scale analysis. Cities, 85, 1–14.

Sharifi, A., Wu, Y., Khamchiangta, D., Yoshida, T., & Yamagata, Y. (2018). Urban carbon mapping: Towards a standardized framework. Energy Procedia, 152, 799–808.

Shen, Y., Kong, W., Fei, F., Chen, X., Xu, Y., Huang, C., & Yao, J. (2024). Stereoscopic urban morphology metrics enhance the nonlinear scale heterogeneity modeling of UHI with explainable AI. Urban Climate, 56, Article 102006.

Silva, R., Eggimann, S., Fierz, L., Fiorentini, M., Orehounig, K., & Baldini, L. (2022). Opportunities for passive cooling to mitigate the impact of climate change in Switzerland. Building and Environment, 208, Article 108574.

Song, H., Cervini, G., Shreevastava, A., & Jung, J. (2024). Reshaping landscape factorization through 3D landscape clustering for urban temperature studies. Sustainable Cities and Society, 115, Article 105809.

Stewart, I. D., & Oke, T. R. (2009). Classifying urban climate field sites by "local climate zones": The case of Nagano, Japan. In IN: Seventh International Conference on Urban Climate (p. 29).

Stewart, I. D., & Oke, T. R. (2012). Local climate zones for urban temperature studies. Bulletin of the American Meteorological Society, 93(12), 1879–1900.

Sun, C., Zhang, Y., Ma, W., Wu, R., & Wang, S. (2022). The impacts of urban form on carbon emissions: A comprehensive review. Land, 11(9), 1430.

Tu, D., Tang, J., Zhang, Z., & Sun, H. (2023). Thermal environment optimization in a large space building for energy-saving. Case Studies in Thermal Engineering, 51, Article 103649.

Wang, D. (2010). Studies on Net Carbon Reserves in Beijing Urban Landscape Green Based on Biomass Measurement. Beijing, China: Beijing Forestry University. PhD Thesis.

Wang, G., Han, Q., & de Vries, B. (2020). A geographic carbon emission estimating framework on the city scale. Journal of Cleaner Production, 244, Article 118793.

Wang, J., Huang, W., & Biljecki, F. (2024). Learning visual features from figure-ground maps for urban morphology discovery. Computers, Environment and Urban Systems, 109, Article 102076.

Wang, J., Liu, W., Sha, C., Zhang, W., Liu, Z., Wang, Z., … Du, X. (2023). Evaluation of the impact of urban morphology on commercial building carbon emissions at the block scale–A study of commercial buildings in Beijing. Journal of Cleaner Production, 408, 137191.

Wang, N., Jusuf, K., Syafii, N., Chen, Y., Hajadi, N., Sathyanarayanan, H., & Manickavasagam, Y. (2011). Evaluation of the impact of the surrounding urban morphology on building energy consumption. Solar Energy, 85(1), 57–71.

Wilson, E., Nicol, F., Nanayakkara, L., & Ueberjahn-Tritta, A. (2008). Public urban open space and human thermal comfort: The implications of alternative climate

change and socio-economic scenarios. Journal of Environmental Policy and Planning, 10(1), 31–45.

Wu, Y., Sharifi, A., Yang, P., Borjigin, H., Murakami, D., & Yamagata, Y. (2018). Mapping building carbon emissions within local climate zones in Shanghai. Energy Procedia, 152, 815–822.

Xia, B., & Zhang, H. (2018). Summarization of research on the guidance and control methods of low-carbon urban blocks. Huazhong Architecture, 36(9), 12–15.

Xie, M., Wang, M., Zhong, H., Li, X., Li, B., Mendis, T., & Xu, S. (2023). The impact of urban morphology on the building energy consumption and solar energy generation potential of university dormitory blocks. Sustainable Cities and Society, 96, Article 104644.

Xin, M., & Feng, S. (2024). Urban rail transit network topology evolutionary stage has influence on rail ridership: Insights from linear mixed-effects models with heterogeneity in variances. Transportation Research Part A, 180, Article 103951.

Xu, S., Wang, S., Li, G., Zhou, H., Meng, C., Qin, Y., & He, B. J. (2024). Performancebased design of residential blocks for the co-benefits of building energy efficiency and outdoor thermal comfort improvement. Building and Environment, 264, Article 111926.

Xu, X., Ou, J., Liu, P., Liu, X., & Zhang, H. (2021). Investigating the impacts of three dimensional spatial structures on CO2 emissions at the urban scale. Science of the Total Environment, 762, Article 143096.

Xuan, W. (2021). Research on reducing carbon consumption in residential community spaces as influenced by microclimate environments. Journal of Urban Planning and Development-ASCE, 147, Article 04021037.

Yang, G., Fu, Y., Yan, M., & Zhang, J. (2020). Exploring the distribution of energy consumption in a northeast Chinese city based on local climate zone scheme: Shenyang city as a case study. Energy Exploration & Exploitation, 38(5), 2079–2094.

Yang, J., Su, J., Xia, J., Jin, C., Li, X., & Ge, Q. (2018). The impact of spatial form of urban architecture on the urban thermal environment: A case study of the Zhongshan district, Dalian, China. IEEE Journal of Selected Topics in Applied Earth Observations and Remote Sensing, 11(8), 2709–2716.

Yang, X., Peng, L. L., Jiang, Z., Chen, Y., Yao, L., He, Y., & Xu, T. (2020). Impact of urban heat island on energy demand in buildings: Local climate zones in Nanjing. Applied Energy, 260, Article 114279.

Yang, Y., Hsieh, C., & Wu, X. (2024). How the urban morphology affects the suitable solar energy techniques and performance: A block-scale study based on the typological method in Macau. Solar Energy, 275, Article 112620.

Yang, Y., Zhang, X., Lu, X., Hu, J., Pan, X., Zhu, Q., & Su, W. (2017). Effects of building design elements on residential thermal environment. Sustainability, 10(1), 57.

Ye, H., Li, Y., Shi, D., Meng, D., Zhang, N., & Zhao, H. (2023). Evaluating the potential of achieving carbon neutrality at the neighborhood scale in urban areas. Sustainable Cities and Society, 97, Article 104764.

Ye, Z., & Wang, J. (2015). Carbon Accounting for Chinese Cities Green District Plans: Methodology, Data and Evaluation Guidelines. Beijing, China: China Architecture & Building Press.

Zhang, R., Matsushima, K., & Kobayashi, K. (2018). Can land use planning help mitigate transport-related carbon emissions? A case of Changzhou. Land Use Policy, 74, 32–40.

Zhang, X., Chen, H., Sun, J., & Zhang, X. (2024). Predictive models of embodied carbon emissions in building design phases: Machine learning approaches based on residential buildings in China. Building and Environment, 258, Article 111595.

Zheng, F., Wang, Y., Shen, Z., & Wang, Y. (2023). Research on the Correlations between Spatial Morphological Indices and Carbon Emission during the Operational Stage of Built Environments for Old Communities in Cold Regions. Buildings, 13(9), 2222.

Zheng, S., Huang, Y., & Sun, Y. (2022). Effects of urban form on carbon emissions in China: implications for low-carbon urban planning. Land, 11(8), 1343.

Zheng, Y., Ren, C., Xu, C., Ho, J., Lau, K., & Ng, E. (2018). GIS–based mapping of Local Climate Zone in the high-density city of Hong Kong. Urban Climate, 24(08), 419–448.

Zhou, L., & Zhang, Y. (2021). A case of shanghai downtown area research on correlation between microclimate environment, assessment and urban form in high-density urban block. Urbanism and Architecture, 18(22), 27–32.

Zhu, X. H., Lu, K. F., Peng, Z. R., He, H. D., & Xu, S. Q. (2022). Spatiotemporal variations of carbon dioxide (CO2) at Urban neighborhood scale: Characterization of distribution patterns and contributions of emission sources. Sustainable Cities and Society, 78, 103646.